J Artif Organs (2009) 12:17–22
DOI 10.1007/s10047-008-0438-z

© The Japanese Society for Artificial Organs 2009

MINIREVIEW

Toru Kawada, MD, PhD · Masaru Sugimachi, MD, PhD

Artificial neural interfaces for bionic cardiovascular treatments

Abstract An artificial nerve, in the broad sense, may be conceptualized as a physical and logical interface system that reestablishes the information traffic between the central nervous system and peripheral organs. Studies on artificial nerves targeting the autonomic nervous system are in progress to explore new treatment strategies for several cardiovascular diseases. In this article, we will review our research targeting the autonomic nervous system to treat cardiovascular diseases. First, we identified the rule for decoding native sympathetic nerve activity into a heart rate using transfer function analysis, and established a framework for a neurally regulated cardiac pacemaker. Second, we designed a bionic baroreflex system to restore the baroreflex buffering function using electrical stimulation of the celiac ganglion in a rat model of orthostatic hypotension. Third, based on the hypothesis that autonomic imbalance aggravates chronic heart failure, we implanted a neural interface into the right vagal nerve and demonstrated that intermittent vagal stimulation significantly improved the survival rate in rats with chronic heart failure following myocardial infarction. Although several practical problems need to be resolved, such as those relating to the development of electrodes feasible for long-term nerve activity recording, studies of artificial neural interfaces with the autonomic nervous system have great possibilities in the field of cardiovascular treatment. We expect further development of artificial neural interfaces as novel strategies to cope with cardiovascular diseases resistant to conventional therapeutics.

Received: June 24, 2008

T. Kawada (✉) · M. Sugimachi
Department of Cardiovascular Dynamics, Advanced Medical Engineering Center, National Cardiovascular Center Research Institute, Osaka 565-8565, Japan
Tel. +81-6-6833-5012; Fax +81-6-6835-5403
e-mail: torukawa@res.ncvc.go.jp

Part of this article is a translation of an article in Japanese that appeared in *Jinkozoki* 2006;3(3):352–355

Key words Autonomic nervous system · Arterial pressure · Orthostatic hypotension · Heart failure · Transfer function

Introduction

Peripheral nerves are the pathways that convey information from peripheral organs to the central nervous system and commands from the central nervous system to peripheral organs. Damage to the peripheral nerves caused by injury or disease is disadvantageous to living organs. In the narrow sense, an artificial nerve would indicate a replacement of the nerve fiber or nerve bundle with artificial materials capable of conducting nerve impulses. In the broad sense, the artificial nerve may be conceptualized as a physical and logical interface system that reestablishes the information traffic between the central nervous system and peripheral organs. Studies on artificial eyes and ears aim to restore sensory functions by building neural interfaces between artificial sensory devices and sensory nerves, the brainstem, or the sensory cortex.[1–4] Studies on functional electrical stimulation aim to restore motor functions via electrical activation of lower motor neurons through stimulation of axons in peripheral nerves or within the spinal cord.[5] Functional electrical stimulation may also be applied directly to skeletal muscles.[6] In addition to these studies on artificial nerves relating to the sensory and motor systems, studies targeting the autonomic nervous system are in progress to explore new treatment strategies for cardiovascular diseases.

The heart has automaticity, which allows it to continue beating even in the absence of regulation by the autonomic nervous system. Loss of autonomic nervous regulation does not instantly terminate the circulation. In this sense, the significance of studies on artificial nerves targeting the autonomic nervous system to treat cardiovascular diseases may be somewhat elusive compared with studies related to the sensory and motor systems. However, the disruption of the autonomic nervous regulation critically affects the activities

of daily living. As an example, patients with severe orthostatic hypotension cannot maintain adequate arterial pressure to remain conscious during sitting or in the standing position and are forced to become bedridden. An artificial neural interface with the autonomic nervous system is expected to be an effective countermeasure to such diseased conditions. In this article, we will review our research targeting the autonomic nervous system to treat cardiovascular diseases.

Neurally regulated cardiac pacemaker

Regulatory systems in living organs, such as the autonomic nervous system, sense multiple physiological variables and control the effector organs accordingly. The first requirement in the development of an artificial neural interface system that can control effector organs is to decode native neural impulses quantitatively and interpret the commands from the central nervous system to the effector organs. In reference to the sympathetic heart rate control mechanism, although sympathetic activation is known to increase heart rate, a qualitative understanding of the input–output relationship is of little use in the development of a neurally regulated cardiac pacemaker. To examine the input–output relationship between these two variables, we measured left cardiac sympathetic nerve activity and heart rate in anesthetized rabbits.[7] The cervical vagal nerves were sectioned to avoid any vagal effects on heart rate. By imposing random pressure variations on the isolated carotid sinuses, we perturbed sympathetic nerve activity via the carotid sinus baroreflex. Plotting the instantaneous heart rate versus sympathetic nerve activity did not reveal any apparent correlations between the two signals (Fig. 1A). This is because the current heart rate is not determined solely by current sympathetic nerve activity but is also influenced by the past history of sympathetic nerve activity.

To identify the dynamic input–output relationship between sympathetic nerve activity and heart rate, including the effect of past history, we employed a white noise analysis used in the engineering field (see Appendix A for details). The transfer function from sympathetic nerve activity to heart rate approximated a low-pass filter (Fig. 1B). The response of the heart rate became smaller and more delayed as the frequency of input perturbation increased. Berger et al. identified similar low-pass-filterlike characteristics of sympathetic heart rate control using random electrical stimulation of the cardiac sympathetic nerve in anesthetized dogs.[8] When we calculated the impulse response via the inverse Fourier transform of the transfer function (see Appendix A for details), the impulse response revealed a significant positive value for approximately 10 s. This result indicates that sympathetic nerve activity at any given time influences heart rate for approximately 10 s in rabbits (Fig. 1B). Once the impulse response is obtained, we can predict the output signal (heart rate) from the convolution integral between the input signal (sympathetic nerve activity) and the impulse response. The heart rate predicted from the measured sympathetic nerve activity demonstrated good agreement with the measured heart rate (Fig. 1C). Although several practical problems need to be resolved, accurate prediction of the instantaneous heart rate makes the transfer function approach extremely attractive as a principle for designing a neurally regulated cardiac pacemaker.

Here we further discuss transfer function analysis to aid in-depth understanding. In the above-mentioned study,[7] we calculated the transfer function from left cardiac sympathetic nerve activity to heart rate. In reality, a branch of the left cardiac sympathetic nerve was sectioned and the nerve activity was recorded from the proximal end of the sectioned nerve. Therefore, the sympathetic nerve from which activity was recorded could not affect heart rate at the time of the experiment. In addition, because the sinus node is predominantly innervated by the right cardiac sympathetic

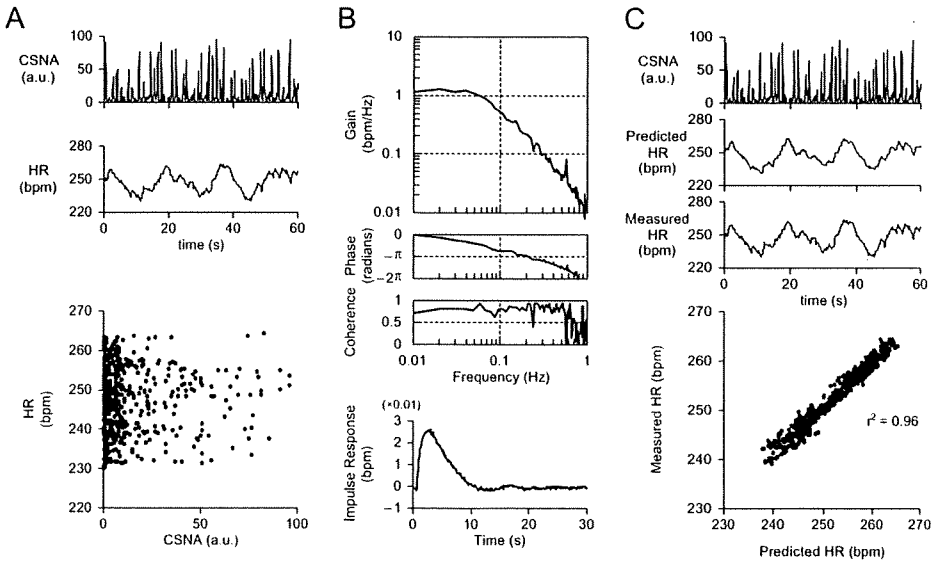

Fig. 1A–C. Decoding of sympathetic heart rate control.[7] **A** Recordings of cardiac sympathetic nerve activity (*CSNA*) and heart rate (*HR*), which were then plotted against each other. **B** Transfer function from CSNA to HR and the corresponding impulse response. **C** Prediction of HR from CSNA using the transfer function. A scatter plot of measured HR versus predicted HR shows the accuracy of this prediction

nerve, changes in heart rate are produced mainly by the right cardiac sympathetic nerve.[9] An implicit assumption of the study is that left cardiac sympathetic nerve activity could be a proxy of the total sympathetic nerve activity that regulates the heart rate. The high coherence between left cardiac sympathetic nerve activity and heart rate is in support of this assumption (Fig. 1B). If the heart rate was regulated by a mechanism totally independent of left cardiac sympathetic nerve activity, the coherence function would have shown values close to zero. We verified our assumption by simultaneously recording left and right cardiac sympathetic nerve activities.[10] There was no apparent laterality of cardiac sympathetic nerve activities in response to dynamic carotid sinus baroreflex perturbation. The laterality observed in the sympathetic effects on the heart rate and ventricular contractility[9] may be mainly attributable to the different distributions of left and right cardiac sympathetic nerves within the heart.

Bionic baroreflex system

Multiple system atrophy (Shy–Drager syndrome) is caused by a disorder of the autonomic nervous system. Shy–Drager patients suffer from severe orthostatic hypotension because of the lack of a baroreflex buffering effect. Although countermeasures to orthostatic hypotension are used, such as administration of pressor agents and volume expansion, these treatments may induce supine hypertension. Ideal treatment would increase arterial pressure only when necessary, i.e., a position-dependent, or more accurately a pressure-dependent, pressor effect is required. In Shy–Drager patients, plasma noradrenaline levels are nearly normal in the supine position and increase following tyramine administration, indicating that peripheral postganglionic sympathetic nerves are relatively spared but only weakly activated by postural changes.[11] If we can encode the information necessary for arterial pressure regulation and deliver those signals to the postganglionic sympathetic system, orthostatic hypotension may be prevented using artificial sympathetic neural interventions.

Because a single nerve fiber discharges according to the all-or-nothing principle, it conveys information by frequency modulation. In contrast, multiple-fiber recording of a nerve bundle exhibits both frequency and amplitude modulations. This is because the amplitude of multiple-fiber recording is the weighted sum of concurrently discharging nerve impulses in the nerve bundle. Nerve fibers adjacent to the electrodes will contribute more to the amplitude generation. The ultimate goal of an artificial neural interface would be to create a respective interface with each nerve fiber in the bundle that could reproduce both the frequency and amplitude modulations. It is unrealistic at present, however, to establish such a complete interface, given the large number of nerve fibers and the small size of the interface.

An alternative strategy for neural interventions is to create a single neural interface to the whole nerve bundle and to treat the system from nerve bundle stimulation to the effector response as a peripheral effector system. Using the electrical stimulation of the celiac ganglion, we explored the development of an artificial vasomotor center to restore normal arterial baroreflex function in rats with central baroreflex failure.[12,13] We first identified the dynamic characteristics of the carotid sinus baroreflex by imposing random pressure perturbations on the isolated carotid sinuses. The transfer function from baroreceptor pressure input to arterial pressure is defined as the native baroreflex function $[H_{Native}(f)]$. Next, we imposed random electrical stimulations on the celiac ganglion and quantified the transfer function from electrical stimulation to the arterial pressure response $[H_{Stim\rightarrow AP}(f)]$. Because the celiac ganglion governs a large abdominal vascular bed, electrical stimulation of the celiac ganglion effectively increased arterial pressure. The transfer function of the controller $[H_{Bionic}(f)]$ was then determined in the frequency domain to fulfill the following equation (Fig. 2A, see Appendix B for details):

$$H_{Bionic}(f)H_{Stim\rightarrow AP}(f) = H_{Native}(f)$$

In a typical experimental result (Fig. 2B), a head-up tilt did not decrease arterial pressure substantially in a rat with a normal baroreflex. In contrast, the same head-up tilt caused significant hypotension in a rat with baroreflex failure. Activation of the bionic baroreflex system was able to restore the baroreflex buffering to a degree similar to that observed in the rat with a normal baroreflex.

Note that native neural discharge of the celiac ganglion was not recorded to develop the bionic baroreflex system,[12,13] whereas recording of the native cardiac sympathetic nerve activity was essential for the development of a neurally regulated cardiac pacemaker.[7] This distinction comes from the fact that the artificial vasomotor center was designed to control the peripheral effector system via electrical stimulation of the celiac ganglion to exert an arterial pressure response. A variety of interventions capable of changing arterial pressure can be treated as a peripheral effector of the bionic baroreflex system. We identified the transfer function from epidural spinal cord stimulation to the arterial pressure response and demonstrated that the bionic baroreflex system using epidural spinal cord stimulation could prevent orthostatic hypotension in anesthetized cats.[14] Yamasaki et al. applied the bionic baroreflex system using epidural spinal cord stimulation to prevent hypotension after sudden deflation of the thigh tourniquet in knee joint surgery.[15] Gotoh et al. demonstrated that an artificial neural interface with the vasomotor center (rostral ventrolateral medulla) provided rapid and precise control of arterial pressure in conscious rats.[16]

Bionic treatment against chronic heart failure

The autonomic nervous system plays an important role in maintaining the circulation under normal physiological conditions. Sympathetic activation and vagal withdrawal during exercise are beneficial to increase cardiac output in response

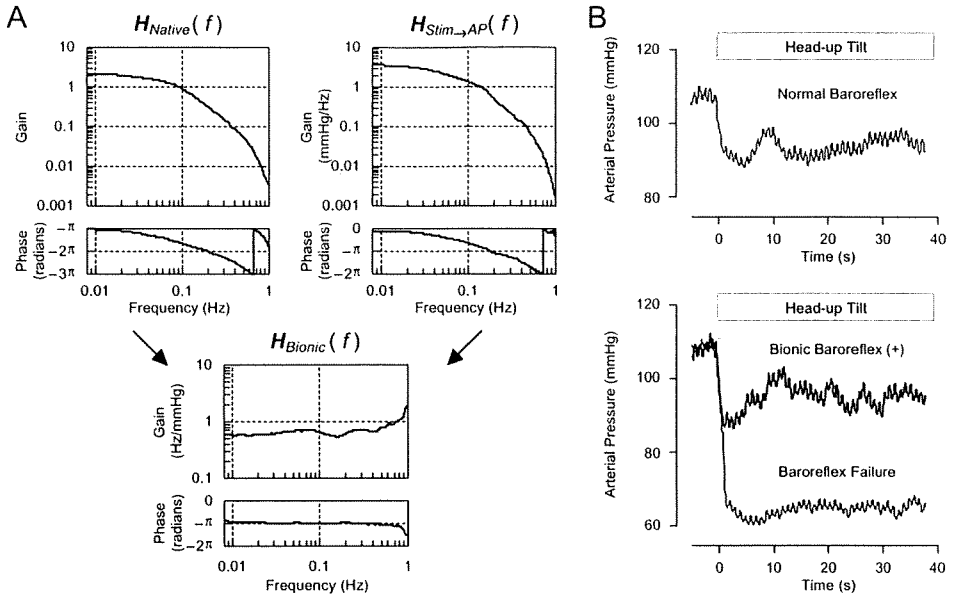

Fig. 2A,B. Arterial pressure regulation by a bionic baroreflex system.[13] **A** Transfer function of the native baroreflex [$H_{Native}(f)$], transfer function from stimulation of the celiac ganglion to arterial pressure [$H_{Stim\rightarrow AP}(f)$], and transfer function of the bionic baroreflex [$H_{Bionic}(f)$]. **B** Arterial pressure responses during a head-up tilt in a rat with normal baroreflex (*top*) and in a rat with central baroreflex failure (*bottom*). Activation of the bionic baroreflex system restored the buffering effect against orthostatic hypotension

to increased oxygen demand. Native autonomic regulation, however, does not always operate properly under disease conditions. Heart failure develops when the heart can no longer provide adequate cardiac output to meet the oxygen demand. While sympathetic activation and vagal withdrawal help compensate for the reduced cardiac performance initially, sympathetic overactivity and vagal withdrawal eventually exacerbate the failing heart, resulting in sympathovagal imbalance and the vicious circle of chronic heart failure. Based on the pathological observation that sympathetic overactivity worsens heart failure, beta-adrenergic blockers and angiotensin converting enzyme inhibitors have been used as treatment. Although beta-blockers were long considered to be contraindicated in heart failure, these drugs were ultimately demonstrated to improve outcome and are now established treatments.[17] Nevertheless, the therapeutic effect of sympathetic blockade is not always sufficient.

We hypothesized that vagal activation would also help terminate the vicious circle in chronic heart failure, and examined whether vagal nerve stimulation could treat chronic heart failure.[18] In halothane-anesthetized rats, the left coronary artery was ligated to produce myocardial infarction. One week later, a telemetry system to record arterial pressure and heart rate and a telestimulator system to stimulate the right vagal nerve were implanted under anesthetized conditions. Another week later (at 14 days after myocardial infarction), surviving rats were divided into vagal stimulation and control groups. In the vagal stimulation group, the right cervical vagal nerve was stimulated intermittently (10-s stimulation per minute) for 6 weeks. The intensity of vagal stimulation was adjusted to decrease the heart rate by 20–30 beats/min. A 140-day follow-up revealed that vagal stimulation significantly increased the survival rate (Fig. 3). Although we did not directly treat the failing heart, the artificial neural interface to the vagal nerve ameliorated heart failure, thereby improved the survival rate.

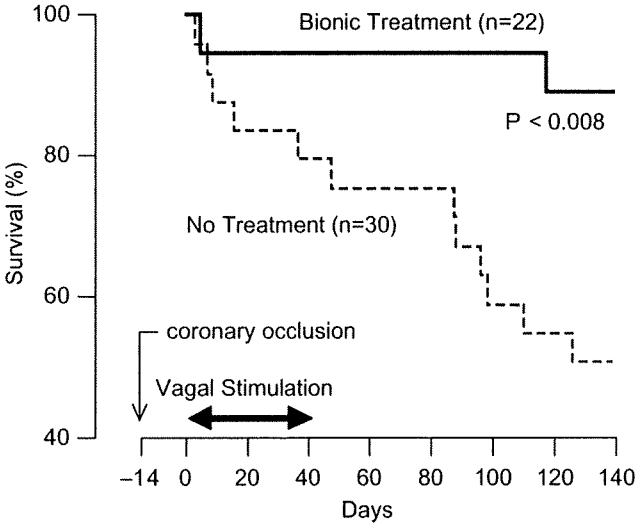

Fig. 3. Survival of rats with chronic heart failure after myocardial infarction.[18] Vagal stimulation dramatically improved the survival rate

The mechanisms by which vagal stimulation ameliorates chronic heart failure are not fully understood. Because vagal stimulation decreases heart rate, myocardial oxygen consumption is reduced. Vagal stimulation can also reduce ventricular contractility via antagonism of the sympathetic effect,[19] which may also help reduce myocardial oxygen demand. Vagal stimulation shows an antifibrillatory effect during ischemic insult in healed myocardial infarction in conscious dogs.[20] In acute myocardial ischemia, vagal stimulation reduces the accumulation of noradrenaline in the myocardial interstitium of the ischemic region.[21] Because catecholamines have cardiotoxicity,[22] reducing myocardial interstitial noradrenaline levels in the ischemic region may be cardioprotective. Vagal stimulation also reduces the

protein levels of endogenous active matrix metalloproteinase-9 during ischemia–reperfusion injury,[23] which may contribute to the inhibition of ventricular remodeling. Because acetylcholine concentrations in the ischemic myocardium are increased via a local releasing mechanism that is independent of voltage-dependent calcium channels,[24,25] vagal stimulation can only induce small additional increases in acetylcholine concentrations in the ischemic region.[21] Given the profound ameliorative effect of vagal stimulation in chronic heart failure,[18] the target of the vagal effect may be the ischemic border zone, rather than the ischemic zone itself. Also, the vagal afferent pathway may modify the central nervous system to exert beneficial effects in chronic heart failure. Development of a new experimental method, such as that using reversible vagal blockade in conscious rats,[26] would help separate the afferent and efferent effects of vagal stimulation. Further studies are required to identify the mechanisms of cardioprotection by vagal stimulation.

Conclusion

In this review, we briefly summarized studies of artificial neural interfaces targeting the autonomic nervous system with the goal of treating several cardiovascular diseases. In all of the studies discussed, creating a logical and physical interface with the autonomic nervous system is the key to effective cardiovascular treatment. In relation to the logical interface, we have demonstrated that the application of white noise analysis was useful in decoding and encoding information for the autonomic nervous system. In relation to the physical interface, electrodes truly capable of long-term recording have not yet been realized. Although we examined the application of sieve-type nerve regeneration electrodes for stimulating and recording the autonomic nerves, further refinements are necessary for practical use. Studies of artificial neural interfaces with the autonomic nervous system are intriguing and have immense possibilities in the field of cardiovascular treatment. We expect further development of artificial neural interfaces as novel strategies to manage cardiovascular diseases that are resistant to conventional therapeutics.

Appendix A

Transfer function analysis

We resampled input–output data of sympathetic nerve activity and heart rate at 10 Hz, and segmented them into eight sets of 50%-overlapping bins of 1024 points each. For each segment, the linear trend was subtracted and a Hanning window was applied. A fast Fourier transform was performed to obtain the frequency spectra of the input and output. Ensemble averages of input power spectra $[S_{XX}(f)]$, output power spectra $[S_{YY}(f)]$, and the cross-spectra between the input and output $[S_{YX}(f)]$ were then calculated. The transfer function was estimated from the following equation:[27]

$$H(f)=\frac{S_{YX}(f)}{S_{XX}(f)} \tag{A1}$$

The coherence function between the input and output was calculated from the following equation:[27]

$$Coh(f)=\frac{|S_{YX}(f)|^2}{S_{XX}(f)S_{YY}(f)} \tag{A2}$$

The coherence function ranges from zero to unity. Zero coherence indicates total independence between the input and output. Unity coherence indicates a perfect linear dependence of the output on the input.

Once the transfer function was identified, we could calculate the impulse response of the system $[h(\tau)]$ via inverse Fourier transform of the transfer function. We then predicted the system response $[y(t)]$ to an input signal $[x(t)]$ from the convolution integral between $h(\tau)$ and $x(t)$ according to the following equation:

$$y(t)=\int_0^T h(\tau)x(t-\tau)d\tau \tag{A3}$$

Although the above convolution integral predicts changes in the output signal in response to changes in the input signal, it cannot usually predict the direct current component or mean value of the output signal. In the case of sympathetic heart rate control, the heart rate does not become zero in the absence of sympathetic stimulation. In the prediction (Fig. 1C), we added the mean value of the measured heart rate to the output signal of the convolution integral to predict the absolute heart rate value.

Appendix B

Designing a bionic baroreflex system

The transfer function of the native baroreflex $[H_{Native}(f)]$ determined the dynamic input–output relationship between baroreceptor pressure input $[P_{Input}(f)]$ and arterial pressure $[AP(f)]$ in the frequency domain:

$$AP(f)=H_{Native}(f)P_{Input}(f) \tag{B1}$$

The transfer function from the stimulus command to the arterial pressure $[H_{Stim\rightarrow AP}(f)]$ determined the dynamic input–output relationship between the stimulus command $[C_{Stim}(f)]$ and arterial pressure in the frequency domain:

$$AP(f)=H_{Stim\rightarrow AP}(f)C_{Stim}(f) \tag{B2}$$

The transfer function of the bionic baroreflex $[H_{Bionic}(f)]$ determined the dynamic input–output relationship between the baroreceptor pressure input and the stimulus command in the frequency domain:

$$C_{Stim}(f)=H_{Bionic}(f)P_{Input}(f) \tag{B3}$$

From equations B2 and B3, arterial pressure regulation by the bionic baroreflex can be described as follows:

$$AP(f) = H_{Stim \rightarrow AP}(f) H_{Bionic}(f) P_{Input}(f) \quad \text{(B4)}$$

Comparison of Eqs. B1 and B4 shows that the bionic baroreflex should fulfill the following equation to reproduce the native baroreflex function:

$$H_{Bionic}(f) = \frac{H_{Native}(f)}{H_{Stim \rightarrow AP}(f)} \quad \text{(B5)}$$

After determining the transfer function of the bionic baroreflex, we obtained the impulse response of the bionic baroreflex system $[h_{Bionic}(\tau)]$ via inverse Fourier transform of the transfer function. We then calculated the stimulus command $[c_{Stim}(t)]$ from the convolution integral between $h_{Bionic}(\tau)$ and the baroreceptor pressure input $[p_{Input}(t)]$, according to the following equation:

$$c_{Stim}(f) = \int_0^T h_{Bionic}(\tau) p_{Input}(t-\tau) d\tau \quad \text{(B6)}$$

In the above convolution integral, $p_{Input}(t)$ was treated as the change in arterial pressure from the arterial pressure value measured immediately before hypotensive intervention.

Acknowledgments This work was supported in part by a Health and Labour Sciences Research Grant for Research on Advanced Medical Technology, a Health and Labour Sciences Research Grant for Research on Medical Devices for Analyzing, Supporting and Substituting the Function of the Human Body, and a Health and Labour Sciences Research Grant from the Ministry of Health, Labour and Welfare of Japan (H18-Iryo-Ippan-023, H19-Nano-Ippan-009).

References

1. Dowling J. Artificial human vision. Expert Rev Med Devices 2005;2:73–85
2. Walter P, Kisvárday ZF, Görtz M, Alteheld N, Rossler G, Stieglitz T, Eysel UT. Cortical activation via an implanted wireless retinal prosthesis. Invest Ophthalmol Vis Sci 2005;46(5):1780–1785
3. Papsin BC, Gordon KA. Cochlear implants for children with severe-to-profound hearing loss. N Engl J Med 2007;357:2380–2387
4. Lim HH, Lenarz T, Joseph G, Battmer RD, Samii A, Samii M, Patrick JF, Lenarz M. Electrical stimulation of the midbrain for hearing restoration: insight into the functional organization of the human central auditory system. J Neurosci 2007;27:13541–13551
5. Mushahwar VK, Jacobs PL, Normann RA, Triolo RJ, Kleitman N. New functional electrical stimulation approaches to standing and walking. J Neural Eng 2007;4(3):S181–S197
6. Sujith OK. Functional electrical stimulation in neurological disorders. Eur J Neurol 2008;15:437–444
7. Ikeda Y, Sugimachi M, Yamasaki T, Kawaguchi O, Shishido T, Kawada T, Alexander J Jr, Sunagawa K. Explorations into development of a neurally regulated cardiac pacemaker. Am J Physiol 1995;269:H2141–H2146
8. Berger RD, Saul JP, Cohen RJ. Transfer function analysis of autonomic regulation. I. Canine atrial rate response. Am J Physiol 1989;256:H142–H152
9. Miyano H, Nakayama Y, Shishido T, Inagaki M, Kawada T, Sato T, Miyashita H, Sugimachi M, Alexander J Jr, Sunagawa K. Dynamic sympathetic regulation of left ventricular contractility studied in the isolated canine heart. Am J Physiol 1998;275: H400–H408
10. Kawada T, Uemura K, Kashihara K, Jin Y, Li M, Zheng C, Sugimachi M, Sunagawa K. Uniformity in dynamic baroreflex regulation of left and right cardiac sympathetic nerve activities. Am J Physiol Regul Integr Comp Physiol 2003;284:R1506–R1512
11. Parikh SM, Diedrich A, Biaggioni I, Robertson D. The nature of the autonomic dysfunction in multiple system atrophy. J Neurol Sci 2002;200:1–10
12. Sato T, Kawada T, Shishido T, Sugimachi M, Alexander J Jr, Sunagawa K. Novel therapeutic strategy against central baroreflex failure: a bionic baroreflex system. Circulation 1999;100:299–304
13. Sato T, Kawada T, Sugimachi M, Sunagawa K. Bionic technology revitalizes native baroreflex function in rats with baroreflex failure. Circulation 2002;106:730–734
14. Yanagiya Y, Sato T, Kawada T, Inagaki M, Tatewaki T, Zheng C, Kamiya A, Takaki H, Sugimachi M, Sunagawa K. Bionic epidural stimulation restores arterial pressure regulation during orthostasis. J Appl Physiol 2004;97:984–990
15. Yamasaki F, Ushida T, Yokoyama T, Ando M, Yamashita K, Sato T. Artificial baroreflex: clinical application of a bionic baroreflex system. Circulation 2006;113:634–639
16. Gotoh TM, Tanaka K, Morita H. Controlling arterial blood pressure using a computer–brain interface. Neuroreport 2005;16: 343–347
17. Mudd JO, Kass DA. Tackling heart failure in the twenty-first century. Nature 2008;451:919–928
18. Li M, Zheng C, Sato T, Kawada T, Sugimachi M, Sunagawa K. Vagal nerve stimulation markedly improves long-term survival after chronic heart failure in rats. Circulation 2004;109:120–124
19. Nakayama Y, Miyano H, Shishido T, Inagaki M, Kawada T, Sugimachi M, Sunagawa K. Heart rate-independent vagal effect on end-systolic elastance of the canine left ventricle under various levels of sympathetic tone. Circulation 2001;104:2277–2279
20. Vanoli E, De Ferrari GM, Stramba-Badiale M, Hull SS Jr, Foreman RD, Schwartz PJ. Vagal stimulation and prevention of sudden death in conscious dogs with a healed myocardial infarction. Circ Res 1991;68:1471–1481
21. Kawada T, Yamazaki T, Akiyama T, Li M, Ariumi H, Mori H, Sunagawa K, Sugimachi M. Vagal stimulation suppresses ischemia-induced myocardial interstitial norepinephrine release. Life Sci 2006;78:882–887
22. Rona G. Catecholamine cardiotoxicity. J Mol Cell Cardiol 1985; 17:291–306
23. Uemura K, Li M, Tsutsumi T, Yamazaki T, Kawada T, Kamiya A, Inagaki M, Sunagawa K, Sugimachi M. Efferent vagal nerve stimulation induces tissue inhibitor of metalloproteinase-1 in myocardial ischemia–reperfusion injury in the rabbit. Am J Physiol Heart Circ Physiol 2007;293:H2254–H2261
24. Kawada T, Yamazaki T, Akiyama T, Sato T, Shishido T, Inagaki M, Takaki H, Sugimachi M, Sunagawa K. Differential acetylcholine release mechanisms in the ischemic and non-ischemic myocardium. J Mol Cell Cardiol 2000;32:405–414
25. Kawada T, Yamazaki T, Akiyama T, Uemura K, Kamiya A, Shishido T, Mori H, Sugimachi M. Effects of Ca^{2+} channel antagonists on nerve stimulation-induced and ischemia-induced myocardial interstitial acetylcholine release in cats. Am J Physiol Heart Circ Physiol 2006;291:H2187–H2191
26. Zheng C, Kawada T, Li M, Sato T, Sunagawa K, Sugimachi M. Reversible vagal blockade in conscious rats using a targeted delivery device. J Neurosci Methods 2006;156:71–75
27. Marmarelis PZ, Marmarelis VZ. Analysis of physiological systems. The white noise method in system identification. New York: Plenum, 1978;131–221

J Physiol Sci (2009) 59:447–455
DOI 10.1007/s12576-009-0055-5

ORIGINAL PAPER

High levels of circulating angiotensin II shift the open-loop baroreflex control of splanchnic sympathetic nerve activity, heart rate and arterial pressure in anesthetized rats

Toru Kawada · Atsunori Kamiya · Meihua Li · Shuji Shimizu · Kazunori Uemura · Hiromi Yamamoto · Masaru Sugimachi

Received: 21 May 2009 / Accepted: 19 July 2009 / Published online: 18 August 2009
© The Physiological Society of Japan and Springer 2009

Abstract Although an acute arterial pressure (AP) elevation induced by intravenous angiotensin II (ANG II) does not inhibit sympathetic nerve activity (SNA) compared to an equivalent AP elevation induced by phenylephrine, there are conflicting reports as to how circulating ANG II affects the baroreflex control of SNA. Because most studies have estimated the baroreflex function under closed-loop conditions, differences in the rate of input pressure change and the magnitude of pulsatility may have biased the estimation results. We examined the effects of intravenous ANG II (10 μg kg^{-1} h^{-1}) on the open-loop system characteristics of the carotid sinus baroreflex in anesthetized and vagotomized rats. Carotid sinus pressure (CSP) was raised from 60 to 180 mmHg in increments of 20 mmHg every minute, and steady-state responses in systemic AP, splanchnic SNA and heart rate (HR) were analyzed using a four-parameter logistic function. ANG II significantly increased the minimum values of AP (67.6 ± 4.6 vs. 101.4 ± 10.9 mmHg, $P < 0.01$), SNA (33.3 ± 5.4 vs. 56.5 ± 11.5%, $P < 0.05$) and HR (391.1 ± 13.7 vs. 417.4 ± 11.5 beats/min, $P < 0.01$). ANG II, however, did not attenuate the response range for AP (56.2 ± 7.2 vs. 49.7 ± 6.2 mmHg), SNA (69.6 ± 5.7 vs. 78.9 ± 9.1%) or HR (41.7 ± 5.1 vs. 51.2 ± 3.8 beats/min). The maximum gain was not affected for AP (1.57 ± 0.28 vs. 1.20 ± 0.25), SNA (1.94 ± 0.34 vs. 2.04 ± 0.42%/mmHg) or HR (1.11 ± 0.12 vs. 1.28 ± 0.19 beats min^{-1} $mmHg^{-1}$). It is concluded that high levels of circulating ANG II did not attenuate the response range of open-loop carotid sinus baroreflex control for AP, SNA or HR in anesthetized and vagotomized rats.

Keywords Systems analysis · Open-loop gain · Equilibrium diagram · Carotid sinus baroreflex · Rats

T. Kawada (✉) · A. Kamiya · M. Li · S. Shimizu · K. Uemura · M. Sugimachi
Department of Cardiovascular Dynamics, Advanced Medical Engineering Center, National Cardiovascular Center Research Institute, 5-7-1 Fujishirodai, Suita, Osaka 565-8565, Japan
e-mail: torukawa@res.ncvc.go.jp

M. Li · S. Shimizu
Japan Association for the Advancement of Medical Equipment, Tokyo 113-0033, Japan

H. Yamamoto
Division of Cardiology, Department of Internal Medicine, Kinki University School of Medicine, Osaka 589-8511, Japan

Introduction

The arterial baroreflex is an important negative feedback system that stabilizes systemic arterial pressure (AP) during daily activities. The sympathetic arterial baroreflex can be divided into the neural and peripheral arc subsystems [1]. The neural arc characterizes the input–output relation between the baroreceptor pressure input and efferent sympathetic nerve activity (SNA), whereas the peripheral arc defines the input–output relation between SNA and AP. These subsystems operate as a controller and a plant, respectively, in the negative feedback loop. Although the input signal to the neural arc is primarily the absolute input pressure level, the rate of input pressure change [1–3] and the magnitude of pulsatility [4–7] are also important input signals that critically affect the baroreflex function. Many investigators employ pharmacologic interventions, such as intravenous phenylephrine and nitroprusside administration, to estimate baroreflex function under closed-loop conditions. The rate of input pressure change and the

magnitude of pulsatility, however, may vary within and between studies, which could bias the estimation results. In addition, experiments performed under baroreflex closed-loop conditions do not usually permit an evaluation of the baroreflex control of AP, because measured AP cannot be separated into signals for the input pressure and output pressure. An open-loop experiment with isolated baroreceptor regions is therefore required to evaluate the baroreflex function precisely.

Angiotensin II (ANG II) can affect the arterial baroreflex by centrally increasing sympathetic outflow, stimulating sympathetic ganglia and the adrenal medulla, and facilitating neurotransmission at sympathetic nerve endings [8]. Although an acute AP elevation induced by intravenous ANG II does not inhibit SNA compared to an equivalent AP elevation induced by phenylephrine, how circulating ANG II affects the baroreflex control of SNA varies among reports, i.e., intravenous ANG has been shown to attenuate [9, 10] or not attenuate [11, 12] the baroreflex control of SNA. Because it is related to the pathologic sympathoexcitation observed in such cardiovascular diseases as chronic heart failure [13], analyzing the effects of circulating ANG II on the baroreflex open-loop system characteristics will deepen our understanding of the pathologic roles of ANG II. In the present study, we examined the effects of intravenous ANG II (10 $\mu g\ kg^{-1}\ h^{-1}$ or 167 $ng\ kg^{-1}\ min^{-1}$) on the open-loop system characteristics of the baroreflex neural and peripheral arcs in anesthetized rats. We hypothesized that ANG II would increase the minimum SNA and attenuate the range of SNA response because the maximum SNA may be saturated. Contrary to our hypothesis, ANG II increased both the minimum and maximum SNA, preserving the range of SNA response controlled by the arterial baroreflex.

Materials and methods

Animals were cared for in strict accordance with the guiding principles for the care and use of animals in the field of physiological sciences, which has been approved by the Physiological Society of Japan. All experimental protocols were reviewed and approved by the Animal Subjects Committee at the National Cardiovascular Center.

Baroreflex open-loop experiment

Male Sprague–Dawley rats ($n = 8$, 482 ± 14 g body weight, mean ± SE) were anesthetized with an intraperitoneal injection (2 ml/kg) of a mixture of urethane (250 mg/ml) and α-chloralose (40 mg/ml), and mechanically ventilated with oxygen-enriched room air. A venous catheter was inserted into the right femoral vein, and a tenfold dilution of the anesthetic mixture was administered ($2\ ml\ kg^{-1}\ h^{-1}$) to maintain an appropriate level of anesthesia. An arterial catheter was inserted into the right femoral artery to measure AP. A cardiotachometer was used to measure heart rate (HR). Another venous catheter was inserted into the left femoral vein to administer Ringer's solution with or without ANG II.

We exposed a postganglionic branch of the splanchnic nerve through a left flank incision and attached a pair of stainless steel wire electrodes (Bioflex wire AS633, Cooner Wire, CA) to record SNA. The nerve and electrodes were covered with silicone glue (Kwik-Sil, World Precision Instruments, Sarasota, FL) for insulation and fixation. To quantify the nerve activity, the preamplified nerve signal was band-pass filtered at 150–1,000 Hz, and then full-wave rectified and low-pass filtered with a cutoff frequency of 30 Hz. Pancuronium bromide ($0.4\ mg\ kg^{-1}\ h^{-1}$) was administered to prevent muscular activity from contaminating the SNA recording. At the end of the experiment, we confirmed the disappearance of SNA after an intravenous bolus injection of hexamethonium bromide (60 mg/kg) and recorded the noise level.

The vagal and aortic depressor nerves were sectioned at the neck to avoid reflexes from the cardiopulmonary region and aortic arch. The bilateral carotid sinuses were isolated from the systemic circulation according to previously reported procedures [14, 15]. Briefly, a fine needle with a 7-0 polypropylene suture (PROLENE, Ethicon, GA, USA) was passed through the tissue between the external and internal carotid arteries, and the external carotid artery was ligated close to the carotid bifurcation. The internal carotid artery was embolized using two or three bearing balls (0.8 mm in diameter, Tsubaki Nakashima, Nara, Japan), which were injected from the common carotid artery. The isolated carotid sinuses were filled with warmed Ringer's solution through catheters inserted via the common carotid arteries. Carotid sinus pressure (CSP) was controlled using a servo-controlled piston pump. Heparin sodium (100 U/kg) was given intravenously to prevent blood coagulation. Body temperature was maintained at approximately 38°C with a heating pad.

Protocols

Sympathetic nerve activity and AP responses to CSP perturbations were monitored for at least 30 min after the surgical preparation was completed. If these responses became smaller within this period, the animal was discarded from the study. Possible causes for deteriorations in the responses include surgical damage to the carotid sinus nerves and brain ischemia due to bilateral carotid occlusion.

The CSP was decreased to 60 mmHg for 4–6 min, and then increased every minute from 60 to 180 mmHg using 20-mmHg increments. At least four step cycles were performed under control conditions while Ringer's solution was continuously administered (6 ml kg^{-1} h^{-1}). After recording the control data, the intravenous Ringer's solution was replaced with that containing ANG II (167 ng kg^{-1} min^{-1}). The dose of ANG II was chosen to induce a significant pressor effect based on previous studies [16, 17]. At least three step cycles were performed during ANG II administration.

Data analysis

Data were sampled at 200 Hz using a 16-bit analog-to-digital converter and stored on the hard disk of a dedicated laboratory computer system. To quantify the open-loop static characteristics of the carotid sinus baroreflex, mean values of SNA, AP and HR were calculated during the last 10 s at each CSP level. The effects of ANG II were assessed during the third step cycle after ANG II administration began, at which point the hemodynamic responses to ANG II appeared to reach steady state. Comparisons were made against two control step cycles (control 1 and control 2, see Fig. 1). In each animal, the SNA noise level recorded after the administration of hexamethonium bromide was set to zero. The SNA values obtained at a CSP level of 60 mmHg during control 1 and control 2 were averaged and defined as 100%.

The open-loop characteristics of the AP, SNA and HR responses as functions of CSP were quantified by fitting a four-parameter logistic function to the obtained data as follows [18]:

$$y = \frac{P_1}{1 + \exp[P_2(\mathrm{CSP} - P_3)]} + P_4.$$

where y represents AP, SNA or HR; P_1 is the response range (the difference between the maximum and minimum values of y); P_2 is a slope coefficient; P_3 is the midpoint in CSP; P_4 is the minimum value of y. The maximum gain or maximum slope of the sigmoidal curve was obtained from $P_1P_2/4$.

The open-loop characteristics of the baroreflex peripheral arc (i.e., SNA–AP relation) were quantified using linear regression analysis as follows:

$$\mathrm{AP} = a \times \mathrm{SNA} + b.$$

where a and b represent the slope and intercept of the regression line, respectively.

Statistical analysis

All parameters were compared among control 1, control 2 and ANG II conditions using repeated-measures analysis of variance [19]. When there was a significant difference among the three conditions, all pairwise comparisons were performed using the Student-Neuman-Keuls test. Differences were considered significant at $P < 0.05$. All data are expressed as mean and SE values.

Results

Typical experimental recordings are shown in Fig. 1. The stepwise input from 60 to 180 mmHg was imposed repeatedly on CSP. An increase in CSP decreased SNA. m-SNA represents the 5-s moving-average signal of the percentage of SNA. AP and HR were also decreased in response to increases in CSP. After ANG II administration was initiated, the levels of SNA, AP and HR all increased compared to the levels before ANG II administration. The responses in SNA, AP and HR to the CSP input appeared to be preserved. Data obtained from the three boxes with dashed lines (control 1, control 2 and ANG II) were used for the statistical analysis.

The open-loop characteristics of the total baroreflex revealed sigmoidal nonlinearity (Fig. 2a). No significant differences were observed between the two control conditions. ANG II significantly increased the minimum AP without affecting the response range, slope coefficient or midpoint in CSP (Table 1). The maximum gain of the total baroreflex was unchanged. The open-loop characteristics of the baroreflex control of HR also approximated sigmoidal nonlinearity (Fig. 2b), and no significant differences were observed between the two control conditions. ANG II significantly increased the minimum HR without affecting the response range, slope coefficient or midpoint in CSP (Table 1). The maximum slope of the baroreflex control of HR was unchanged.

The total baroreflex was decomposed into the neural and peripheral arc subsystems. The open-loop characteristics of the baroreflex neural arc revealed sigmoidal nonlinearity (Fig. 3a). There were no significant differences between the two control conditions. ANG II significantly increased the minimum SNA (Table 1). Although the midpoint in CSP was lower in ANG II than in control 1, the difference was not significant when compared with control 2. ANG II did not affect the response range, slope coefficient or the maximum slope of the baroreflex control of SNA. The open-loop characteristics of the baroreflex peripheral arc approximated a straight line (Fig. 3b). There were no significant differences between the two control conditions. ANG II significantly increased the intercept of the regression line (Table 1). AP at 100% SNA did not change significantly, suggesting that the slope of the regression line could be shallower under the ANG II condition. The slope of the

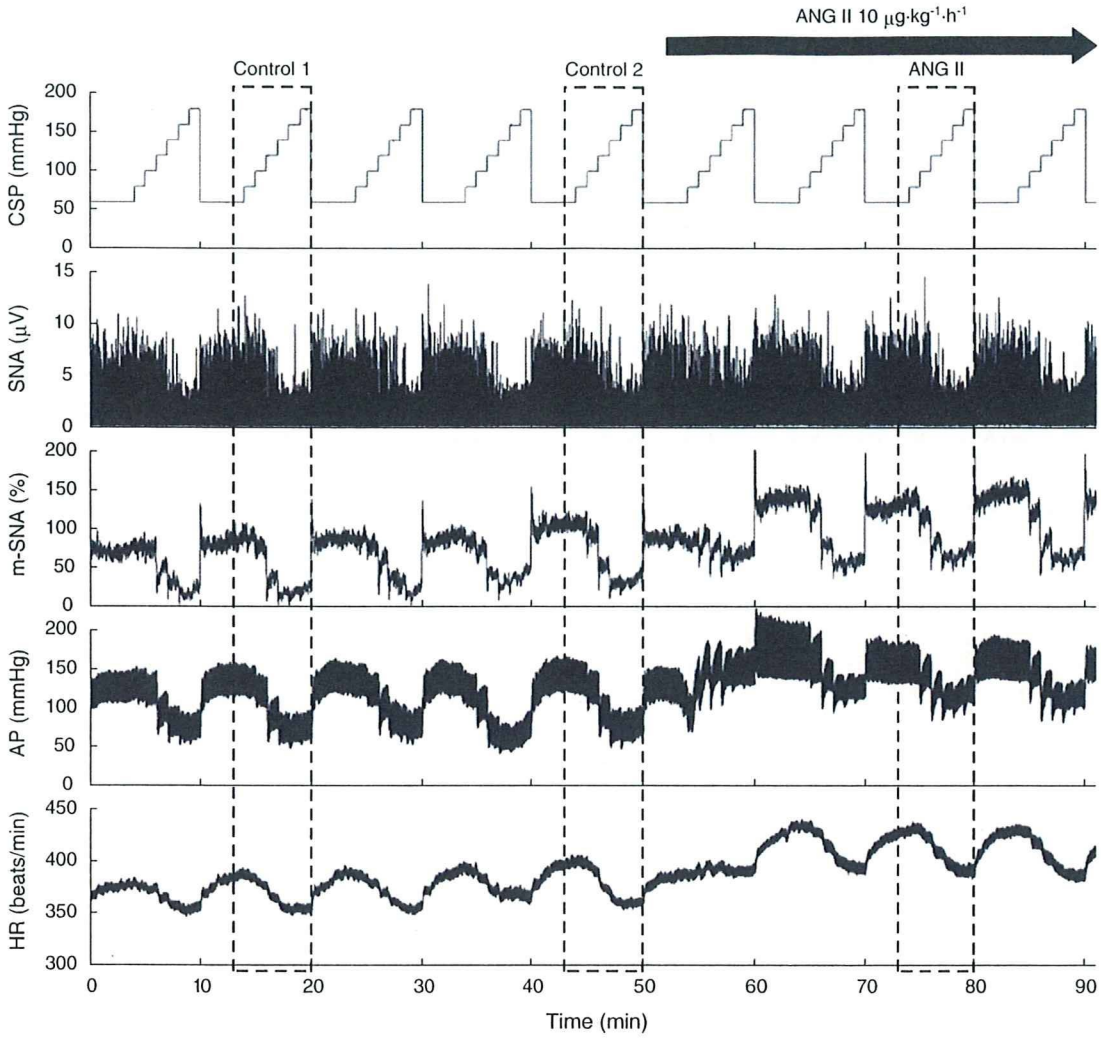

Fig. 1 Typical recordings of carotid sinus pressure (*CSP*), splanchnic sympathetic nerve activity (*SNA*), the 5-s moving-average signal of the percentage of SNA (*m-SNA*), systemic arterial pressure (*AP*) and heart rate (*HR*). CSP was changed stepwise from 60 to 180 mmHg in 20-mmHg increments every minute. Angiotensin II (ANG II) was administered intravenously while the CSP perturbation was continued. ANG II significantly increased SNA, AP and HR. Reflex responses in SNA, AP and HR were not attenuated in the presence of ANG II. *Dashed boxes* indicate the step cycles used for the statistical analysis

regression line, however, was not statistically different among the three conditions.

An equilibrium diagram or a balance diagram was obtained by drawing the neural and peripheral arcs using SNA as the common abscissa and CSP or AP as an ordinate [20–22]. Figure 4 illustrates the equilibrium diagrams under the control 2 (dashed line) and ANG II (solid line) conditions, which were drawn based on the mean parameter values from the logistic function and regression line. Open and filled circles represent the closed-loop operating points under the control 2 and ANG II conditions, respectively. Although AP at the closed-loop operating point was significantly increased by the intravenous ANG II, SNA at the closed-loop operating point was unchanged (Table 1). If ANG II affected the peripheral arc alone, the closed-operating point may have been located at the point depicted by the open triangle. If ANG II affected the neural arc alone, the closed-loop operating point may have been located at the point depicted by the filled triangle.

Discussion

Effects of ANG II on open-loop baroreflex control of SNA

Intravenous ANG II at 167 ng kg^{-1} min^{-1} shifted the open-loop baroreflex control of splanchnic SNA toward higher SNA values without attenuating the size of the response range (Fig. 3a; Table 1). The maximum slope was

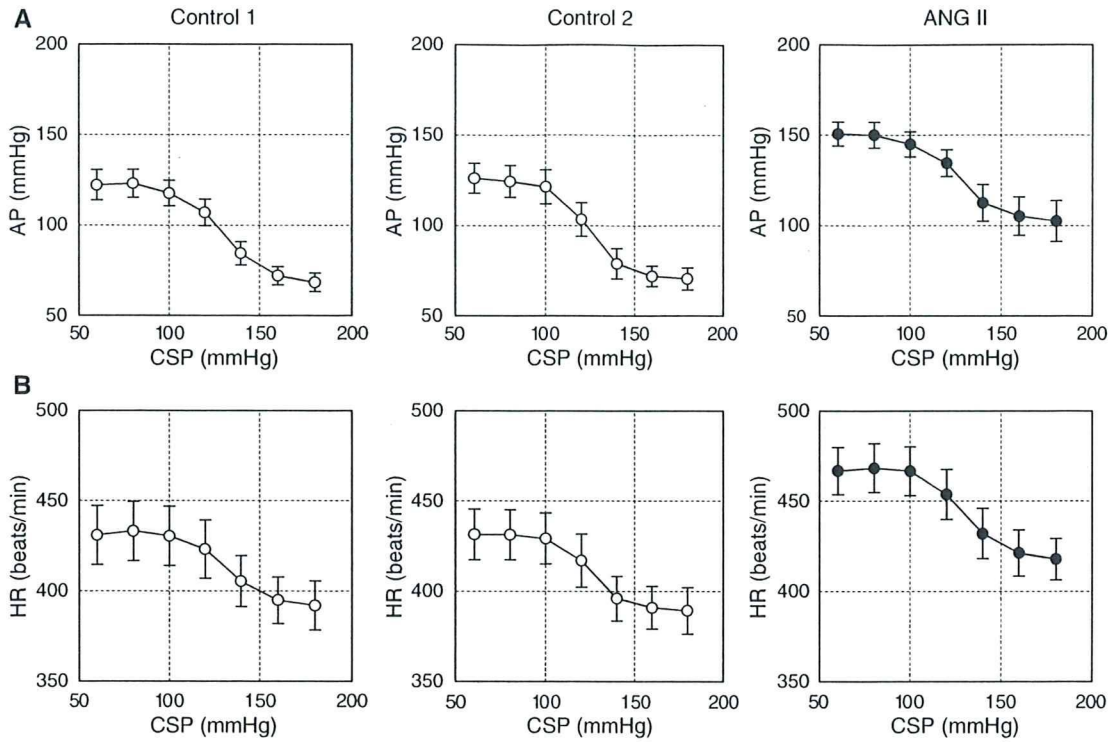

Fig. 2 **a** Averaged input–output relation of the total baroreflex. AP decreased in response to an increase in the CSP. ANG II increased AP, while the range of the AP response was preserved. **b** Averaged input–output relation of the arterial baroreflex control of HR. HR decreased in response to an increase in the CSP. ANG II increased the HR, while the range of the HR response was preserved

unaltered, which agreed with a previous study from our laboratory in which intravenous ANG II at 100 ng kg^{-1} min^{-1} did not change the dynamic gain of the neural arc in anesthetized rabbits [23]. In contrast, Sanderford and Bishop demonstrated that ANG II at 10 or 20 ng kg^{-1} min^{-1} significantly reduced the maximum renal SNA and attenuated the range of baroreflex control of renal SNA in conscious rabbits [9, 24]. On the other hand, Tan et al. [12] demonstrated that intravenous ANG II at 400 ng kg^{-1} min^{-1} did not increase the levels of renal SNA in anesthetized rats. The regional differences in SNA may partly explain the conflicting results, because Fukiyama [25] noted that ANG II infusion (3.5–9.5 ng kg^{-1} min^{-1}) through the vertebral artery resulted in an increase in splanchnic SNA, a transient increase followed by a decrease in renal SNA, and no change in cardiac SNA in anesthetized dogs.

Activation of the renin–angiotensin system contributes to the pathologic sympathoexcitation observed in such cardiovascular diseases as chronic heart failure. In addition to the augmented cardiac sympathetic reflex, impairment of the arterial baroreflex is thought to contribute to sympathoexcitation [13]. The present results indicate that ANG II may increase SNA, but it does not attenuate baroreflex control of SNA such that the magnitude of the SNA response to the input pressure change is preserved (Fig. 3a). ANG II also did not attenuate the gain of the total baroreflex estimated by the magnitude of the AP response to the input pressure change (Fig. 2a). Therefore, the observed weakening of the baroreflex reported in patients with chronic heart failure may not be readily explainable by an acute effect of high circulating levels of ANG II.

Several studies have demonstrated that ANG II-induced hypertension does not decrease SNA via the arterial baroreflex compared to equivalent hypertension induced by phenylephrine [10, 12, 26]. Although those results seem to be consistent with the idea that ANG II blunts the arterial baroreflex, the experimental protocol is confusing, and the interpretation could be wrong as follows. The intersection between the neural and peripheral arcs in the baroreflex equilibrium diagram conforms to the closed-loop operating point [21, 27, 28]. In the present study, ANG II significantly increased AP without significant changes in SNA at the closed-loop operating point (Fig. 4, open vs. filled circles; Table 1). If we calculate the baroreflex control of SNA based on ANG II-induced hypertension, therefore, we would incorrectly conclude that the baroreflex does not control SNA. If we observe the SNA response to changes in

Table 1 Effects of intravenous angiotensin II (ANG II) on the parameters of logistic functions and regression lines of the open-loop baroreflex characteristics

	Control 1	Control 2	ANG II
Total baroreflex, CSP–AP relation			
P_1 (mmHg)	56.2 ± 7.2	56.3 ± 6.4	49.7 ± 6.2
P_2 (mmHg^{-1})	0.116 ± 0.019	0.118 ± 0.015	0.094 ± 0.013
P_3 (mmHg)	129.2 ± 3.5	124.5 ± 2.8	125.7 ± 3.2
P_4 (mmHg)	67.6 ± 4.6	69.7 ± 5.8	101.4 ± 10.9**,††
Maximum gain	1.57 ± 0.28	1.58 ± 0.22	1.20 ± 0.25
Baroreflex control of HR, CSP–HR relation			
P_1(beats/min)	41.7 ± 5.1	43.9 ± 6.2	51.2 ± 3.8
P_2 (mmHg^{-1})	0.123 ± 0.027	0.133 ± 0.018	0.099 ± 0.013
P_3 (mmHg)	131.8 ± 3.8	125.8 ± 3.6	129.1 ± 2.6
P_4 (beats/min)	391.1 ± 13.7	388.0 ± 12.6	417.4 ± 11.5**,††
Maximum slope (beats min^{-1} mmHg^{-1})	1.11 ± 0.12	1.39 ± 0.23	1.28 ± 0.19
Neural arc, CSP–SNA relation			
P_1 (%)	69.6 ± 5.7	66.5 ± 7.4	78.9 ± 9.1
P_2 (mmHg^{-1})	0.110 ± 0.016	0.124 ± 0.015	0.098 ± 0.011
P_3 (mmHg)	133.2 ± 3.8	127.3 ± 3.1	126.0 ± 3.4*
P_4 (%)	33.3 ± 5.4	35.0 ± 6.4	56.5 ± 11.5*,†
Maximum slope (%/mmHg)	1.94 ± 0.34	2.02 ± 0.33	2.04 ± 0.42
Peripheral arc, SNA–AP relation			
Slope, a (mmHg/%)	0.85 ± 0.09	0.86 ± 0.06	0.66 ± 0.10
Intercept, b (mmHg)	37.8 ± 5.2	36.9 ± 5.5	68.0 ± 10.6**,††
AP at 100% SNA (mmHg)	122.7 ± 9.9	122.7 ± 7.0	134.4 ± 4.9
Operating point			
AP (mmHg)	111.4 ± 5.0	110.3 ± 5.1	128.1 ± 4.4**,††
SNA (%)	90.6 ± 7.4	85.8 ± 2.1	94.3 ± 5.9

Data are mean and SE values

CSP Carotid sinus pressure, *AP* arterial pressure, *HR* heart rate, *SNA* sympathetic nerve activity

* $P < 0.05$ and ** $P < 0.01$ from control 1, † $P < 0.05$ and †† $P < 0.01$ from control 2

CSP, however, the baroreflex should be able to control SNA in the presence of ANG II (Fig. 3a). Lumbers et al. [29] pointed out a problem regarding the use of ANG II-induced hypertension as an input perturbation to evaluate the baroreflex.

Effects of ANG II on the baroreflex peripheral arc

The open-loop system characteristics of the baroreflex peripheral arc, assessed using the AP response as a function of SNA, approximated a straight line under both control and ANG II-treated conditions (Fig. 3b), suggesting that the splanchnic SNA may represent changes in systemic SNA that controlled the AP. ANG II significantly increased the intercept of the regression line, reflecting its direct vasoconstrictive effect (Table 1). Because the AP at 100% SNA did not differ among the three conditions, the slope could be shallower in the presence of ANG II. In other words, ANG II appears to elevate the AP to a greater extent for the lower SNA range. Although both the modulation of sympathetic neurotransmission and direct vasoconstriction contribute to the elevation of AP, the fact that ANG II enhances the sympathetic neurotransmission more with a lower stimulation frequency [30, 31] may, in part, account for the greater ANG II-induced increase in AP for the lower SNA range.

Effects of ANG II on the open-loop sympathetic baroreflex control of HR

The baroreflex control of HR showed changes similar to those observed for SNA. Intravenous ANG II increased both the minimum and maximum HR while not significantly affecting the response range of HR or the maximum slope of the response (Fig. 2b; Table 1). The midpoint in CSP was not changed by ANG II. Therefore, the open-loop baroreflex control of HR shifted upward to higher HR values without a concomitant rightward shift to higher CSP values in the present study. In contrast, previous studies reported a rightward shift in the baroreflex control of HR toward higher input pressure values during acute [11, 32] and chronic [33] administration of ANG II in conscious rabbits. Reid and Chou [32] indicated that the inhibition of vagal tone to the heart played a significant role in resetting the baroreflex control of HR in conscious rabbits. It is likely that the rightward shift in the baroreflex control of

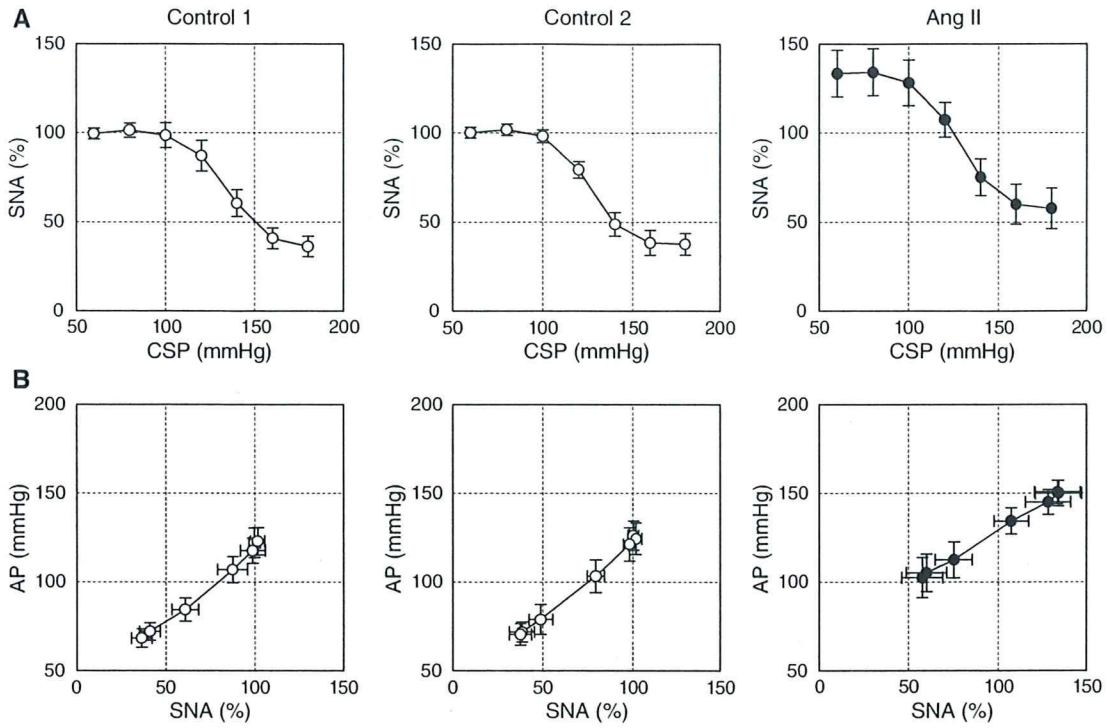

Fig. 3 **a** Averaged input–output relation of the baroreflex neural arc or the arterial baroreflex control of SNA. SNA decreased in response to an increase in the CSP. ANG II increased SNA, while the range of the SNA response was preserved. **b** Averaged input–output relation of the baroreflex peripheral arc. AP increased in response to an increase in SNA. ANG II increased the AP, an effect that was greater for lower SNA

HR by ANG II was not observed in the present study because the vagal nerves were sectioned.

Limitations

First, we performed the experiments in anesthetized animals, and comparisons with results obtained in conscious animals should be made carefully. Circulating levels of ANG II may vary under anesthesia, which could have affected the present results. For instance, reported plasma ANG II concentration in pithed rats is approximately 400 pg/ml [16], which exceeds the plasma ANG II concentration reported in rats with heart failure [34]. Second, although the dose of ANG II used in the present study was within or below those used in previous studies in rats [12, 16, 17], Brown et al. demonstrated that intravenous ANG II at 20 and 270 ng kg^{-1} min^{-1} increased the plasma ANG II concentration from approximately 80 pg/ml to 140 and 2,000 pg/ml, respectively [35]. Based on those data, the plasma ANG II concentration might have been increased beyond a physiologically relevant range to approximately 1,200 pg/ml in the present study. Therefore, the observed effect of ANG II on the arterial baroreflex should be interpreted as pharmacologic. Effects of circulating ANG II can be different when examined in different doses. Third, there was large variation in HR values among the animals (Fig. 2b). Increasing the number of animals would reduce this variation. Nevertheless, data from the eight rats was sufficient to perform statistical analyses and draw reasonable conclusions. Fourth, we occluded the common carotid arteries to isolate the carotid sinuses. Although the vertebral arteries were kept intact and the effects of ANG II were examined using the same preparation, the possibility cannot be ruled out that the carotid occlusion affected the present results. Finally, we cut the vagal nerves to obtain the open-loop condition for the carotid sinus baroreflex. Further studies are needed to clarify the effects of ANG II on the baroreflex control of the cardiovascular system through the vagal system.

Conclusion

The present study indicates that high circulating levels of ANG II significantly increased splanchnic SNA but did not acutely attenuate the range of arterial baroreflex control of SNA. The ranges of the total baroreflex response and the baroreflex control of HR were also preserved during ANG

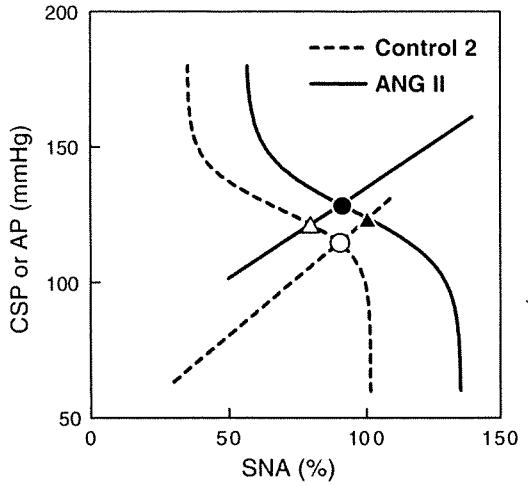

Fig. 4 Equilibrium diagrams between the arterial baroreflex neural and peripheral arcs. The *dashed* and *solid curves* represent the open-loop characteristics of the baroreflex neural arc under the control and ANG II-treated conditions, respectively. The *dashed* and *solid lines* represent the open-loop characteristics of the baroreflex peripheral arc under the control and ANG II-treated conditions, respectively. The *open circle* indicates the closed-loop operating point under the control condition. ANG II causes an upward shift in the peripheral arc. If ANG II does not affect the neural arc, the closed-loop operating point would be at the point depicted by the *open triangle*. In this case, the estimation of baroreflex control of SNA based on the closed-loop operating points (the *open circle* and *open triangle*) approximates the slope of the baroreflex neural arc (*dashed curve*). ANG II, however, causes a rightward shift in the neural arc. Thus, the estimation of the baroreflex control of SNA based on closed-loop operating points (the *open* and *filled circles*) does not match the slope of the neural arc under either the control (*dashed curve*) or ANG II-treated condition (*solid curve*)

II administration. ANG II does modify the arterial baroreflex in that it increases SNA at a given baroreceptor pressure level but does not appear to attenuate the range of arterial baroreflex control of SNA, HR or AP.

Acknowledgments This study was supported by Health and Labour Sciences Research Grants (H18-nano-Ippan-003, H19-nano-Ippan-009, H20-katsudo-Shitei-007, and H21-nano-Ippan-005) from the Ministry of Health, Labour and Welfare of Japan; by a Grant-in-Aid for Scientific Research (No. 20390462) from the Ministry of Education, Culture, Sports, Science and Technology of Japan; and by the Industrial Technology Research Grant Program from the New Energy and Industrial Technology Development Organization (NEDO) of Japan.

References

1. Ikeda Y, Kawada T, Sugimachi M, Kawaguchi O, Shishido T, Sato T, Miyano H, Matsuura W, Alexander J Jr, Sunagawa K (1996) Neural arc of baroreflex optimizes dynamic pressure regulation in achieving both stability and quickness. Am J Physiol 271:H882–H890
2. Kawada T, Yamamoto K, Kamiya A, Ariumi H, Michikami D, Shishido T, Sunagawa K, Sugimachi M (2005) Dynamic characteristics of carotid sinus pressure-nerve activity transduction in rabbits. Jpn J Physiol 55:157–163
3. Sato T, Kawada T, Shishido T, Miyano H, Inagaki M, Miyashita H, Sugimachi M, Kneupfer MM, Sunagawa K (1998) Dynamic transduction properties of in situ baroreceptors of rabbit aortic depressor nerve. Am J Physiol Heart Circ Physiol 274:H358–H365
4. Chapleau MW, Abboud FM (1987) Contrasting effects of static and pulsatile pressure on carotid baroreceptor activity in dogs. Circ Res 61:648–658
5. Kawada T, Fujiki N, Hosomi H (1992) Systems analysis of the carotid sinus baroreflex system using a sum-of-sinusoidal input. Jpn J Physiol 42:15–34
6. Kawada T, Yanagiya Y, Uemura K, Miyamoto T, Zheng C, Li M, Sugimachi M, Sunagawa K (2002) Input-size dependence of the baroreflex neural arc transfer characteristics. Am J Physiol Heart Circ Physiol 284:H404–H415
7. Kawada T, Zheng C, Yanagiya Y, Uemura K, Miyamoto T, Inagaki M, Shishido T, Sugimachi M, Sunagawa K (2002) High-cut characteristics of the baroreflex neural arc preserve baroreflex gain against pulsatile pressure. Am J Physiol Heart Circ Physiol 282:H1149–H1156
8. Reid IA (1992) Interactions between ANG II, sympathetic nervous system, and baroreceptor reflexes in regulation of blood pressure. Am J Physiol Endocrinol Metab 262:E763–E778
9. Sanderford MG, Bishop VS (2000) Angiotensin II acutely attenuates range of arterial baroreflex control of renal sympathetic nerve activity. Am J Physiol Heart Circ Physiol 279:H1804–H1812
10. McMullan S, Goodchild AK, Pilowsky PM (2007) Circulating angiotensin II attenuates the sympathetic baroreflex by reducing the barosensitivity of medullary cardiovascular neurons in the rat. J Physiol 582:711–722
11. Kumagai K, Reid IA (1994) Angiotensin II exerts differential actions on renal nerve activity and heart rate. Hypertension 24:451–456
12. Tan PS, Killinger S, Horiuchi J, Dampney RA (2007) Baroreceptor reflex modulation by circulating angiotensin II is mediated by AT_1 receptors in the nucleus tractus solitarius. Am J Physiol Regul Integr Comp Physiol 293:R2267–R2278
13. Zucker IH (2006) Novel mechanisms of sympathetic regulation in chronic heart failure. Hypertension 48:1005–1011
14. Shoukas AA, Callahan CA, Lash JM, Haase EB (1991) New technique to completely isolate carotid sinus baroreceptor regions in rats. Am J Physiol Heart Circ Physiol 260:H300–H303
15. Sato T, Kawada T, Miyano H, Shishido T, Inagaki M, Yoshimura R, Tatewaki T, Sugimachi M, Alexander J Jr, Sunagawa K (1999) New simple methods for isolating baroreceptor regions of carotid sinus and aortic depressor nerves in rats. Am J Physiol Heart Circ Physiol 276:H326–H332
16. Grant TL, McGrath JC (1988) Interactions between angiotensin II, sympathetic nerve-mediated pressor response and cyclo-oxygenase products in the pithed rat. Br J Pharmacol 95:1220–1228
17. Haywood JR, Fink GD, Buggy J, Phillips MI, Brody MJ (1980) The area postrema plays no role in the pressor action of angiotensin in the rat. Am J Physiol Heart Circ Physiol 239:H108–H113
18. Kent BB, Drane JW, Blumenstein B, Manning JW (1972) A mathematical model to assess changes in the baroreceptor reflex. Cardiology 57:295–310
19. Glantz SA (2002) Primer of biostatistics, 5th edn. McGraw-Hill, New York
20. Mohrman DE, Heller LJ (2006) Cardiovascular physiology, 6th edn. McGraw Hill, New York, pp 172–177
21. Sato T, Kawada T, Inagaki M, Shishido T, Takaki H, Sugimachi M, Sunagawa K (1999) New analytic framework for

understanding sympathetic baroreflex control of arterial pressure. Am J Physiol Heart Circ Physiol 276:H2251–H2261
22. Kawada T, Shishido T, Inagaki M, Zheng C, Yanagiya Y, Uemura K, Sugimachi M, Sunagawa K (2002) Estimation of baroreflex gain using a baroreflex equilibrium diagram. Jpn J Physiol 52:21–29
23. Kashihara K, Takahashi Y, Chatani K, Kawada T, Zheng C, Li M, Sugimachi M, Sunagawa K (2003) Intravenous angiotensin II does not affect dynamic baroreflex characteristics of the neural or peripheral arc. Jpn J Physiol 53:135–143
24. Sanderford MG, Bishop VS (2002) Central mechanisms of acute ANG II modulation of arterial baroreflex control of renal sympathetic nerve activity. Am J Physiol Heart Circ Physiol 282:H1592–H1602
25. Fukiyama K (1972) Central action of angiotensin and hypertension—increased central vasomotor outflow by angiotensin. Jpn Circ J 36:599–602
26. Guo GB, Abboud FM (1984) Angiotensin II attenuates baroreflex control of heart rate and sympathetic activity. Am J Physiol Heart Circ Physiol 246:H80–H89
27. Kamiya A, Kawada T, Yamamoto K, Michikami D, Ariumi H, Uemura K, Zheng C, Shimizu S, Aiba T, Miyamoto T, Sugimachi M, Sunagawa K (2005) Resetting of the arterial baroreflex increases orthostatic sympathetic activation and prevents postural hypotension in rabbits. J Physiol 566:237–246
28. Yamamoto K, Kawada T, Kamiya A, Takaki H, Miyamoto T, Sugimachi M, Sunagawa K (2004) Muscle mechanoreflex induces the pressor response by resetting the arterial baroreflex neural arc. Am J Physiol Heart Circ Physiol 286:H1382–H1388
29. Lumbers ER, McCloskey DI, Potter EK (1979) Inhibition by angiotensin II of baroreceptor-evoked activity in cardiac vagal efferent nerves in the dog. J Physiol 294:69–80
30. Hughes J, Roth RH (1971) Evidence that angiotensin enhances transmitter release during sympathetic nerve stimulation. Br J Phrmacol 41:239–255
31. Zimmerman BG, Gomer SK, Liao JC (1972) Action of angiotensin on vascular adrenergic nerve endings: facilitation of norepinephrine release. Federation Proc 31:1344–1350
32. Reid IA, Chou L (1990) Analysis of the action of angiotensin II on the baroreflex control of heart rate in conscious rabbits. Endocrinology 126:2749–2756
33. Brooks VL (1995) Chronic infusion of angiotensin II resets baroreflex control of heart rate by an arterial pressure-independent mechanism. Hypertension 26:420–424
34. Schunkert H, Tang SS, Litwin SE, Diamant D, Riegger G, Dzau VJ, Ingelfinger JR (1993) Regulation of intrarenal and circulating renin–angiotensin systems in severe heart failure in the rat. Cardiovasc Res 27:731–735
35. Brown AJ, Casals-Stenzel J, Gofford S, Lever AF, Morton JJ (1981) Comparison of fast and slow pressor effects of angiotensin II in the conscious rat. Am J Physiol Heart Circ Physiol 241:H381–H388

Life Sciences 85 (2009) 597–601

Contents lists available at ScienceDirect

Life Sciences

journal homepage: www.elsevier.com/locate/lifescie

Detection of endogenous acetylcholine release during brief ischemia in the rabbit ventricle: A possible trigger for ischemic preconditioning

Toru Kawada [a,*], Tsuyoshi Akiyama [b], Shuji Shimizu [a], Atsunori Kamiya [a], Kazunori Uemura [a], Meihua Li [a], Mikiyasu Shirai [b], Masaru Sugimachi [a]

[a] Department of Cardiovascular Dynamics, Advanced Medical Engineering Center, National Cardiovascular Center Research Institute, Japan
[b] Department of Cardiac Physiology, National Cardiovascular Center Research Institute, Japan

ARTICLE INFO

Article history:
Received 1 July 2009
Accepted 25 August 2009

Keywords:
Acetylcholine
Cardiac microdialysis
Vagal stimulation
Coronary artery occlusion
Rabbits

ABSTRACT

Aims: To examine endogenous acetylcholine (ACh) release in the rabbit left ventricle during acute ischemia, ischemic preconditioning and electrical vagal stimulation.
Main methods: We measured myocardial interstitial ACh levels in the rabbit left ventricle using a cardiac microdialysis technique. In Protocol 1 ($n=6$), the left circumflex coronary artery (LCX) was occluded for 30 min and reperfused for 30 min. In Protocol 2 ($n=5$), the LCX was temporarily occluded for 5 min. Ten minutes later, the LCX was occluded for 30 min and reperfused for 30 min. In Protocol 3 ($n=5$), bilateral efferent vagal nerves were stimulated at 20 Hz and 40 Hz (10 V, 1-ms pulse duration).
Key findings: In Protocol 1, a 30-min coronary occlusion increased the ACh level from 0.39 ± 0.15 to 7.0 ± 2.2 nM (mean ± SE, $P<0.01$). In Protocol 2, a 5-min coronary occlusion increased the ACh level from 0.33 ± 0.07 to 0.75 ± 0.11 nM ($P<0.05$). The ACh level returned to 0.48 ± 0.10 nM during the interval. After that, a 30-min coronary occlusion increased the ACh level to 2.4 ± 0.49 nM ($P<0.01$). In Protocol 3, vagal stimulation at 20 Hz and 40 Hz increased the ACh level from 0.29 ± 0.06 to 1.23 ± 0.48 ($P<0.05$) and 2.44 ± 1.13 nM ($P<0.01$), respectively.
Significance: Acute ischemia significantly increased the ACh levels in the rabbit left ventricle, which appeared to exceed the vagal stimulation-induced ACh release. Brief ischemia as short as 5 min can also increase the ACh level, suggesting that endogenous ACh release can be a trigger for ischemic preconditioning.
© 2009 Published by Elsevier Inc.

Introduction

Although ventricular vagal innervation is sparser than that observed in the atrium, we have previously demonstrated that electrical vagal stimulation and acute myocardial ischemia significantly increased myocardial interstitial acetylcholine (ACh) levels in the feline left ventricle (Kawada et al. 2000, 2001, 2006a,b, 2007). Potential differences between species, however, suggest that data obtained from the feline left ventricle may not be directly extrapolated to ventricular vagal innervation in other species (Brown 1976; Kilbinger and Löffelholz 1976). Compared with the feline heart, the rabbit heart is more frequently analyzed in investigations of myocardial ischemia and ischemic preconditioning. For instance, Qin et al. (2003) used isolated rabbit hearts to demonstrate that ACh and adenosine induce ischemic preconditioning mimetic effects through different signaling pathways. In our previous study, vagal stimulation increased the level of tissue inhibitor of metalloproteinase-1 (TIMP-1) and reduced the level of endogenous active matrix metalloproteinase-9 (MMP-9) during ischemia–reperfusion injury in the rabbit left ventricle (Uemura et al. 2007). Despite its potential cardioprotective effects against myocardial ischemia, the profile of endogenous ACh release in the rabbit left ventricle is poorly understood *in vivo* owing to the difficulty in detecting low levels of myocardial interstitial ACh. Quantification of endogenous ACh release during myocardial ischemia and electrical vagal stimulation would help understand the potential cardioprotective effects of vagal stimulation. In the present study, we examined the effects of acute myocardial ischemia, ischemic preconditioning, and electrical vagal stimulation on myocardial interstitial ACh levels in the rabbit left ventricle *in vivo* using an improved high-performance liquid chromatography (HPLC) system that allowed us to detect low concentrations of ACh (Shimizu et al. 2009).

Materials and methods

Surgical preparation and protocols

Animal care was conducted in accordance with the *Guiding Principles for the Care and Use of Animals in the Field of Physiological Sciences*, which has been approved by the Physiological Society of

* Corresponding author. Department of Cardiovascular Dynamics, Advanced Medical Engineering Center, National Cardiovascular Center Research Institute, 5-7-1 Fujishirodai, Suita, Osaka 565-8565, Japan. Tel.: +81 6 6833 5012x2427; fax: +81 6 6835 5403.
E-mail address: torukawa@res.ncvc.go.jp (T. Kawada).

0024-3205/$ – see front matter © 2009 Published by Elsevier Inc.
doi:10.1016/j.lfs.2009.08.015

Japan. Japanese white rabbits weighing 2.5 kg to 3.1 kg (2.8 ± 0.1 kg, mean ± SE) were anesthetized via intravenous administration of pentobarbital sodium (30–35 mg/kg) through a marginal ear vein. The animals were ventilated mechanically with room air mixed with oxygen. The anesthetic condition was maintained using a continuous intravenous infusion of urethane (125 mg kg^{-1} h^{-1}) and α-chloralose (20 mg kg^{-1} h^{-1}) through a catheter inserted in the right femoral vein. Mean arterial pressure (AP) was measured using a catheter inserted in the right femoral artery. Heart rate (HR) was measured from an electrocardiogram obtained using a cardiotachometer. The animal was placed in a lateral position, and the left fourth and fifth ribs were partially resected to allow access to the heart. The heart was suspended in a pericardial cradle.

In Protocol 1 ($n = 6$), which was designed to examine the effects of acute myocardial ischemia and reperfusion, a 3-0 silk suture was passed around a branch of the left circumflex coronary artery (LCX); both ends were passed through a polyethylene tube to make a snare to occlude the artery. A dialysis probe was implanted into the anterolateral free wall of the left ventricle perfused by the LCX. After collecting a baseline dialysate sample, the LCX was occluded for 30 min and reperfused for 30 min. After the ischemia–reperfusion protocol was finished, the LCX was occluded again and a 5-ml bolus of 1% methylene blue was injected intravenously to confirm that the dialysis probe had been implanted within the area at risk for myocardial ischemia.

In Protocol 2 ($n = 5$), which was designed to examine the effects of ischemic preconditioning (*i.e.*, a brief ischemic event preceding a major ischemic event), a 3-0 silk suture was passed around a branch of the LCX and both ends were passed through a polyethylene tube to make a snare. Two dialysis probes were implanted into the anterolateral free wall of the left ventricle perfused by the LCX; the probes were separated by at least 5 mm. Combining the dialysate samples obtained from the two dialysis probes increased the time resolution of the ACh measurement. After collecting a baseline dialysate sample, the LCX was temporarily occluded for 5 min which was followed by a 10-min interval. The LCX was then occluded for 30 min and reperfused for 30 min. After the ischemia–reperfusion protocol was completed, the LCX was occluded again and a 5-ml bolus of 1% methylene blue was injected intravenously to confirm that the two dialysis probes had been implanted within the area at risk for myocardial ischemia.

In Protocol 3 ($n = 5$), which was designed to examine the effects of electrical vagal stimulation, the vagus nerves were exposed and sectioned at the neck. Each sectioned vagus nerve was placed on a pair of bipolar platinum electrodes to stimulate the efferent vagus nerve. The nerve and the electrodes were fixed using silicone glue (Kwik-Sil, World Precision Instruments, Sarasota, FL, USA). Two dialysis probes were implanted into the anterolateral free wall of the left ventricle; the probes were separated by at least 5 mm. Dialysate samples obtained from the two dialysis probes were analyzed separately. After collecting baseline dialysate samples, the vagus nerves were stimulated at 20 Hz for 15 min and 40 Hz for 15 min. The stimulation amplitude was 10 V and the pulse duration was 1 ms. The 40-Hz stimulation often caused an initial cardiac arrest for a few seconds and was considered to be the most intensive stimulation in the present experimental settings. The 20-Hz stimulation was arbitrarily selected at a half of the maximum stimulation rate to observe the dependence of the ACh release on the stimulation rate.

At the end of each protocol, the experimental animals were sacrificed with an overdose of intravenous pentobarbital sodium. We performed a postmortem examination and confirmed that the dialysis probe(s) had been implanted within the left ventricular myocardium.

Dialysis technique

We measured dialysate concentrations of ACh as indices of myocardial interstitial ACh levels. The materials and properties of the dialysis probe have been described previously (Akiyama et al. 1994). Briefly, we designed a transverse dialysis probe. A dialysis fiber (length, 8 mm; outer diameter, 310 μm; inner diameter, 200 μm; PAN-1200, 50,000-Da molecular-weight cutoff, Asahi Chemical, Japan) was glued at both ends to polyethylene tubes (length, 25 cm; outer diameter, 500 μm; inner diameter, 200 μm). The dialysis probe was perfused at a rate of 2 μl/min with Ringer's solution containing a cholinesterase inhibitor eserine (100 μM). Dialysate sampling was started from 2 h after probe implantation. In Protocols 1 and 3, one sampling period was set at 15 min, which yielded a sample volume of 30 μl. The actual dialysate sampling lagged behind a given collection period by 5 min owing to the dead space volume between the dialysis membrane and collecting tube. In Protocol 2, one sampling period was set at 5 min to increase the time resolution during the ischemic preconditioning, and dialysate samples from the two dialysis probes were combined to yield a sample volume of 20 μl. The sampling period was changed to 10 min during the main ischemic event to reduce the total number of samples. The amount of ACh in the dialysate was measured using an HPLC system with electrochemical detection (Eicom, Japan) adjusted to measure low levels of ACh (Shimizu et al. 2009). The concentration of ACh was calculated taking the sample volume in account.

Statistical analysis

All data are presented as the mean and SE values. We performed repeated-measures analysis of variance, followed by a Tukey test for all pairwise, multiple comparisons to examine changes in the ACh levels (Glantz 2002). Because the variance of measured ACh levels increased with their mean, statistical analysis was performed after logarithmic conversion of the ACh data (Snedecor and Cochran 1989). The AP and HR data were examined using repeated-measures analysis of variance, followed by a Dunnett's test for multiple comparisons against a single control (Glantz 2002). In Protocols 1 and 3, the baseline value was treated as the single control. In Protocol 2, the value measured just before the main ischemic event was treated as the single control. In all of the statistical analyses, differences were considered significant when $P < 0.05$.

Results

In Protocol 1, the myocardial interstitial ACh levels significantly increased during ischemia compared with the baseline value (Fig. 1). Although the ACh levels declined during reperfusion, they were still significantly higher than the baseline value. Changes in AP and HR are summarized in Table 1. Although AP did not change significantly during ischemia, it decreased significantly throughout the reperfusion period. The HR increased significantly after 30 min of ischemia, and remained high during the reperfusion period with the exception of the last data point.

In Protocol 2, the LCX was occluded for 5 min (ischemic preconditioning) and released for 10 min before the major ischemic event. The brief 5-min occlusion significantly increased the myocardial interstitial ACh level compared with the baseline value (Fig. 2). The ACh levels during the interval between the brief occlusion and the major occlusion did not differ from the baseline value. The ACh levels increased significantly during the major ischemic event compared with the baseline value. Although the ACh levels declined during reperfusion, they were still significantly higher than the baseline value. Changes in AP and HR are summarized in Table 2. Neither AP nor HR changed significantly compared with the respective control values measured after the 10-min middle interval.

In Protocol 3, electrical vagal stimulation significantly increased the myocardial interstitial ACh levels (Fig. 3). The ACh levels returned close to the baseline value just after vagal stimulation was terminated. The AP and HR values were significantly reduced by vagal stimulation (Table 3).

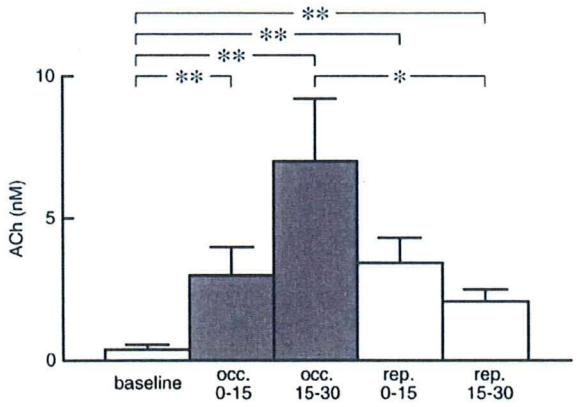

Fig. 1. Changes in the myocardial interstitial ACh levels in Protocol 1. The left circumflex coronary artery was occluded for 30 min and reperfused for 30 min. occ: occlusion; rep: reperfusion. Data are shown as the mean + SE ($n = 6$). $^{*}P < 0.05$ and $^{**}P < 0.01$; Tukey test.

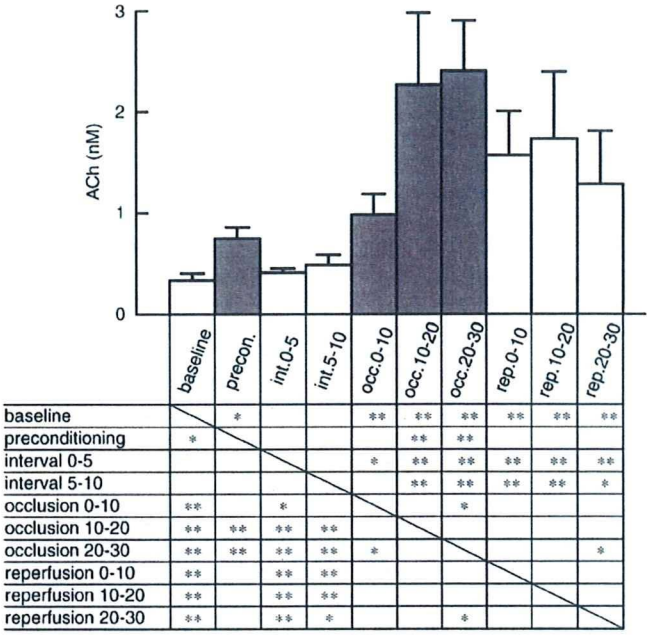

Fig. 2. Changes in the myocardial interstitial ACh levels in Protocol 2. The left circumflex coronary artery was occluded for 5 min. Ten minutes later, the left circumflex coronary artery was occluded for 30 min and reperfused for 30 min. precon: preconditioning; int: interval; occ: occlusion; rep: reperfusion. Data are shown as the mean + SE ($n = 5$). $^{*}P < 0.05$ and $^{**}P < 0.01$; Tukey test.

Discussion

Effects of acute ischemia on myocardial interstitial ACh levels

Acute myocardial ischemia significantly increased myocardial interstitial ACh levels in the ischemic region (Fig. 1). To our knowledge, this is the first report demonstrating ischemia-induced ACh release in the rabbit left ventricle *in vivo*. Because electrical vagal stimulation increased the myocardial interstitial ACh levels (Fig. 3), centrally mediated activation of the efferent vagus nerve could contribute to these effects. LCX occlusion, however, did not decrease the HR significantly (Table 1), suggesting that centrally mediated vagal activation did not have a marked role in the present study. In a previous study, acute myocardial ischemia increased myocardial interstitial ACh levels in vagotomized cats, suggesting an important role of a local release mechanism that is independent of efferent vagal activity (Kawada et al. 2000). Intracellular Ca^{2+} mobilization related to cation-selective stretch-activated channels is thought to be involved in this local release mechanism (Kawada et al. 2000, 2006b). A similar local mechanism may be responsible for ischemia-induced ACh release in the rabbit left ventricle.

In our previous study, topical perfusion of ACh through a dialysis probe increased TIMP-1 levels in the rabbit left ventricle (Uemura et al. 2007). The production of TIMP-1 reduces endogenous levels of active MMP-9, which can limit ventricular remodeling following myocardial ischemia and reperfusion. Whether ischemia-induced ACh release can induce such an anti-remodeling effect remains unanswered, however, because reperfusion reduced the myocardial interstitial ACh levels toward the baseline value. Whether prolonged ischemia for more than 30 min induces sustained elevations of ACh levels is an interesting topic for future studies.

The ACh levels were decreased toward the baseline value upon reperfusion, probably by the washout of ACh from the interstitial fluid. In the case of myocardial interstitial myoglobin levels, the reperfusion further increases the myoglobin levels, suggesting an occurrence of reperfusion injury to the myocardium (Kitagawa et al. 2005). Reoxygenation upon reperfusion rapidly restores the ATP synthesis, which can cause hypercontracture of myofibrils and undesired cytoskeletal lesions (Piper et al. 2004). Because the vagal nerve endings do not have contractile elements, the hypercontracture-induced cell injury does not occur, and the further release of ACh may have been prevented.

Effects of ischemic preconditioning on myocardial interstitial ACh levels

Ischemic preconditioning is a phenomenon in which a brief ischemic event makes the heart resistant to a subsequent ischemic insult (Murry et al. 1986). Acetylcholine, bradykinin, and adenosine are endogenous substances that can induce ischemic preconditioning mimetic effects in the rabbit heart (Liu et al. 1991; Qin et al. 2003; Krieg et al. 2004). In a previous study, we showed that a 5-min ischemic event increased myocardial interstitial ACh levels in the feline ventricle (Kawada et al. 2002). Ischemic preconditioning, however, is not frequently examined in the feline ventricle, making interpretation of these results difficult. In the present study, a 5-min ischemic event caused a significant increase in the ACh level in the rabbit left ventricle (Fig. 2), suggesting that brief ischemia-induced ACh release may serve as a trigger for the ischemic preconditioning. Krieg et al. (2004) demonstrated that ACh triggers preconditioning by sequentially activating Akt and nitric oxide synthase to produce reactive oxygen species. An acetylcholine-induced preconditioning mimetic effect has also been observed in canine (Yao and Gross 1993; Przyklenk and Kloner 1995) and rat (Richard et al. 1995) models.

Table 1
Mean arterial pressure (AP) and heart rate (HR) obtained during Protocol 1 ($n = 6$).

	Baseline	Occlusion 5 min	Occlusion 15 min	Occlusion 30 min	Reperfusion 5 min	Reperfusion 15 min	Reperfusion 30 min
AP(mm Hg)	82 ± 4	77 ± 4	72 ± 5	75 ± 5	72 ± 5*	70 ± 4*	70 ± 2**
HR (beats/min)	247 ± 16	264 ± 14	265 ± 13	280 ± 10**	278 ± 9*	277 ± 8*	274 ± 9

Data are shown as the mean ± SE. $^{*}P < 0.05$ and $^{**}P < 0.01$ vs. baseline using Dunnett's test.

Table 2
Mean arterial pressure (AP) and heart rate (HR) obtained during Protocol 2 ($n=5$).

	Baseline	Preconditioning 5 min	Interval 5 min	Interval 10 min	Occlusion 5 min	Occlusion 10 min
AP(mm Hg)	83±5	77±5	78±4	80±4	78±5	78±5
HR(beats/min)	277±7	282±8	282±7	284±5	285±5	286±6
	Occlusion 20 min	Occlusion 30 min	Reperfusion 5 min	Reperfusion 10 min	Reperfusion 20 min	Reperfusion 30 min
AP(mm Hg)	77±4	78±5	77±5	78±5	77±3	79±3
HR(beats/min)	287±5	289±6	290±5	289±5	290±6	293±5

Data are shown as the mean ± SE. No significant differences relative to control values (the value 10 min after the preconditioning) were observed based on Dunnett's test.

In a previous study examining the feline ventricle (Kawada et al. 2002), brief ischemia significantly decreased the HR, highlighting the presence of a significant vagal reflex from the heart. Vagotomy abolished the ACh release induced by brief ischemia in that study, suggesting an important role of centrally mediated vagal activation. The vagal reflex from the heart, however, shows regional differences and varies among species (Thames et al. 1978; Kawada et al. 2007). In the present study, brief ischemia did not decrease the HR significantly (Table 2), suggesting that centrally mediated vagal activation was not a major factor for the brief ischemia-induced ACh release in the rabbit heart.

Rabbits exhibit marked effects from ischemic preconditioning, including reduced infarct size (Cohen et al. 1991; Cason et al. 1997). Although whether the ACh release induced by the brief ischemic event exerted cardioprotective effects was not examined in the present study, there was a notable difference in the changes in AP observed with Protocol 1 and Protocol 2. Although AP decreased significantly upon reperfusion in Protocol 1 (Table 1), it did not change significantly during the major ischemic event in Protocol 2 (Table 2), possibly reflecting preserved cardiac function as a result of the ischemic preconditioning.

Effects of electrical vagal stimulation on myocardial interstitial ACh levels

In the feline left ventricle, electrical vagal stimulation at 20 Hz (10 V, 1-ms pulse duration) increases myocardial interstitial ACh levels to approximately 20 nM as measured with a dialysis fiber 13 mm in length (Kawada et al. 2000). In contrast, electrical vagal stimulation at 20 Hz in the rabbit left ventricle (10 V, 1-ms pulse duration) increased the ACh levels to approximately 1.2 nM as measured with a dialysis fiber 8 mm long (Fig. 3). The small increase in the ACh level detected during electrical vagal stimulation may indicate that vagal innervation is much sparser in the rabbit ventricle

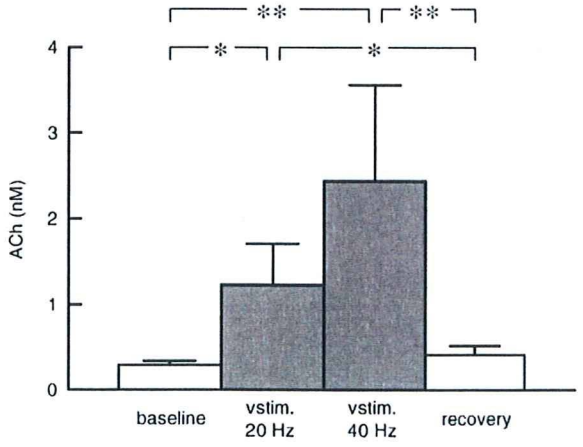

Fig. 3. Changes in the myocardial interstitial ACh levels in Protocol 3. The bilateral efferent vagus nerves were stimulated at 20 Hz for 15 min and 40 Hz for 15 min. Data are shown as the mean + SE ($n=10$, 2 samples from each of the 5 animals). $^{*}P<0.05$ and $^{**}P<0.01$; Tukey test.

than in the feline ventricle. In a previous study that used a dialysis fiber 4 mm in length, right vagal stimulation at 20 Hz increased the dialysate ACh concentration from 0.4±0.2 nM to 0.9±0.3 nM, whereas left vagal stimulation at 20 Hz increased it from 0.3±0.1 nM to 1.0±0.4 nM in the rabbit right ventricle (Shimizu et al. 2009). Considering the bilateral stimulation and fiber length of 8 mm in the present study, the vagal innervation of the left ventricle may be comparable to or slightly sparser than that of the right ventricle.

The dialysis fiber differed in length among studies due to anatomical restrictions related to the fiber implantation procedure (*i.e.*, size of the heart etc.). If we consider diffusive processes alone, the relative recovery (RR) can be expressed as:

$$RR = \frac{C_{inside}}{C_{outside}} = 1-\exp\left(-k\frac{A}{F}\right) = 1-\exp\left(-k\frac{mL}{F}\right)$$

where C_{inside} and $C_{outside}$ are the ACh concentrations inside and outside the dialysis fiber; A is the surface area of the dialysis membrane, which can be proportional to the fiber length L with a coefficient m; F is a perfusion flow rate; and k is the mass transfer coefficient (Ståhle 1991). The *in vitro* RR for ACh is approximately 70% with $F=2$ μl/min and $L=13$ mm (Akiyama et al. 1994), which yields $km=0.1852$. Using this value, the *in vitro* RR would be approximately 52% for $L=8$ mm and 31% for $L=4$ mm. Although these values provide some clues to speculate the effects of fiber length on the detected ACh concentrations, they cannot be directly extrapolated to the present results, because k should be different in *in vivo* conditions.

The physiological significance of vagal innervation of the left ventricle is controversial, because fixed-rate atrial pacing abolishes vagally induced inhibition of left ventricular contractility in an experimental setting without significant background sympathetic tone (Matsuura et al. 1997). On the other hand, when the cardiac sympathetic nerve is activated, vagal stimulation can reduce ventricular contractility even under fixed-rate atrial pacing by antagonizing the sympathetic effect (Nakayama et al. 2001). In addition, vagal stimulation suppresses myocardial interstitial myoglobin release during acute myocardial ischemia in anesthetized cats (Kawada et al. 2008). Chronic vagal stimulation improves the survival rate of rat models of chronic heart failure after myocardial infarction (Li et al. 2004). These lines of evidence suggest that vagal innervation of the left ventricle may be of therapeutic significance.

An unresolved question regarding the cardioprotective effects of vagal stimulation is that a large quantity of ACh is released in the ischemic region without vagal stimulation (Fig. 1). In the present

Table 3
Mean arterial pressure (AP) and heart rate (HR) obtained during Protocol 3 ($n=5$).

	Baseline	Vagal stimulation 20 Hz	Vagal stimulation 40 Hz	Recovery
AP (mm Hg)	100±3	59±9**	54±9**	86±5
HR (beats/min)	322±14	126±5**	100±8**	311±8

Data are shown as the mean ± SE. $^{**}P<0.01$ vs. baseline based on Dunnett's test.

study, vagal stimulation at 20-Hz lowered the HR by approximately 200 beats/min (to less than 40% of the control value) but the stimulation-induced ACh release did not exceed the ischemia-induced ACh release (Figs. 1 and 3). On the other hand, vagal stimulation that reduced the HR by only 10% produces a significant increase in the survival rate of chronic heart failure rats (Li et al. 2004). Therefore, vagal stimulation probably exerts its beneficial effects not only within the ischemic region but also outside of this region. For instance, vagal stimulation in dogs with a healed myocardial infarction is known to prevent lethal arrhythmia induced by exercise (Vanoli et al. 1991). Afferent vagal activation may also contribute to the cardioprotective effects. Further studies are clearly needed to identify the mechanisms underlying the vagally induced cardioprotective effects against myocardial infarction and chronic heart failure.

Conclusion

The present study demonstrated the presence of vagal innervation in the rabbit left ventricle. Acute myocardial ischemia significantly increased the myocardial interstitial ACh levels. In addition, a brief ischemic event (5 min) caused detectable increases in ACh levels, indicating that endogenous ACh release may provide a trigger for ischemic preconditioning.

Acknowledgments

This study was supported by the Health and Labour Sciences Research Grants (H18-nano-Ippan-003, H19-nano-Ippan-009, H20-katsudo-Shitei-007, and H21-nano-Ippan-005) from the Ministry of Health, Labour and Welfare of Japan; by a Grant-in-Aid for Scientific Research (No. 20390462) from the Ministry of Education, Culture, Sports, Science and Technology of Japan; and by the Industrial Technology Research Grant Program from the New Energy and Industrial Technology Development Organization (NEDO) of Japan.

References

Akiyama T, Yamazaki T, Ninomiya I. In vivo detection of endogenous acetylcholine release in cat ventricles. American Journal of Physiology 266 (3 Pt 2), H854–H860, 1994.

Brown OM. Cat heart acetylcholine: Structural proof and distribution. American Journal of Physiology 231 (3), 781–785, 1976.

Cason BA, Gamperl AK, Slocum RE, Hickey RF. Anesthetic-induced preconditioning: Previous administration of isoflurane decreases myocardial infarct size in rabbits. Anesthesiology 87 (5), 1182–1190, 1997.

Cohen MV, Liu GS, Downey JM. Preconditioning causes improved wall motion as well as smaller infarcts after transient coronary occlusion in rabbits. Circulation 84 (1), 341–349, 1991.

Glantz SA. Primer of Biostatistics, 5th ed. McGraw-Hill, New York, 2002.

Kawada T, Yamazaki T, Akiyama T, Sato T, Shishido T, Inagaki M, Takaki H, Sugimachi M, Sunagawa K. Differential acetylcholine release mechanisms in the ischemic and non-ischemic myocardium. Journal of Molecular and Cellular Cardiology 32 (3), 405–414, 2000.

Kawada T, Yamazaki T, Akiyama T, Shishido T, Inagaki M, Uemura K, Miyamoto T, Sugimachi M, Takaki H, Sunagawa K. In vivo assessment of acetylcholine releasing function at cardiac vagal nerve terminals. American Journal of Physiology. Heart and Circulatory Physiology 281 (1), H139–H145, 2001.

Kawada T, Yamazaki T, Akiyama T, Mori H, Inagaki M, Shishido T, Takaki H, Sugimachi M, Sunagawa K. Effects of brief ischaemia on myocardial acetylcholine and noradrenaline levels in anaesthetized cats. Autonomic Neuroscience: Basic and Clinical 95 (1–2), 37–42, 2002.

Kawada T, Yamazaki T, Akiyama T, Li M, Ariumi H, Mori H, Sunagawa K, Sugimachi M. Vagal stimulation suppresses ischemia-induced myocardial interstitial norepinephrine release. Life Sciences 78 (8), 882–887, 2006a.

Kawada T, Yamazaki T, Akiyama T, Uemura K, Kamiya A, Shishido T, Mori H, Sugimachi M. Effects of Ca^{2+} channel antagonists on nerve stimulation-induced and ischemia-induced myocardial interstitial acetylcholine release in cats. American Journal of Physiology. Heart and Circulatory Physiology 291 (5), H2187–H2191, 2006b.

Kawada T, Yamazaki T, Akiyama T, Shishido T, Shimizu S, Mizuno M, Mori H, Sugimachi M. Regional difference in ischaemia-induced myocardial interstitial noradrenaline and acetylcholine releases. Autonomic Neuroscience: Basic and Clinical 137 (1–2), 44–50, 2007.

Kawada T, Yamazaki T, Akiyama T, Kitagawa H, Shimizu S, Mizuno M, Li M, Sugimachi M. Vagal stimulation suppresses ischemia-induced myocardial interstitial myoglobin release. Life Sciences 83 (13–14), 490–495, 2008.

Kilbinger H, Löffelholz K. The isolated perfused chicken heart as a tool for studying acetylcholine output in the absence of cholinesterase inhibition. Journal of Neural Transmission 38, 9–14, 1976.

Kitagawa H, Yamazaki T, Akiyama T, Sugimachi M, Sunagawa K, Mori H. Microdialysis separately monitors myocardial interstitial myoglobin during ischemia and reperfusion. American Journal of Physiology Heart and Circulatory Physiology 289 (2), H924–H930, 2005.

Krieg T, Qin Q, Philipp S, Alexeyev MF, Cohen MV, Downey JM. Acetylcholine and bradykinin trigger preconditioning in the heart through a pathway that induces Akt and NOS. American Journal of Physiology. Heart and Circulatory Physiology 287 (6), H2606–H2611, 2004.

Li M, Zheng C, Sato T, Kawada T, Sugimachi M, Sunagawa K. Vagal nerve stimulation markedly improves long-term survival after chronic heart failure in rats. Circulation 109 (1), 120–124, 2004.

Liu GS, Thornton J, Van Winkle DM, Stanley AW, Olsson RA, Downey JM. Protection against infarction afforded by preconditioning is mediated by A_1 adenosine receptors in rabbit heart. Circulation 84 (1), 350–356, 1991.

Matsuura W, Sugimachi M, Kawada T, Sato T, Shishido T, Miyano H, Nakahara T, Ikeda Y, Alexander Jr J, Sunagawa K. Vagal stimulation decreases left ventricular contractility mainly through negative chronotropic effect. American Journal of Physiology 273 (2 Pt 2), H534–H539, 1997.

Murry CE, Jennings RB, Reimer KA. Preconditioning with ischemia: A delay of lethal cell injury in ischemic myocardium. Circulation 74 (5), 1124–1136, 1986.

Nakayama Y, Miyano H, Shishido T, Inagaki M, Kawada T, Sugimachi M, Sunagawa K. Heart rate-independent vagal effect on end-systolic elastance of the canine left ventricle under various levels of sympathetic tone. Circulation 104 (19), 2277–2279, 2001.

Piper HM, Abdallah Y, Schäfer C. The first minutes of reperfusion: A window of opportunity for cardioprotection. Cardiovascular Research 61 (3), 365–371, 2004.

Przyklenk K, Kloner RA. Low-dose iv acetylcholine acts as a "preconditioning-mimetic" in the canine model. Journal of Cardiac Surgery 10 (4), 389–395, 1995.

Qin Q, Downey JM, Cohen MV. Acetylcholine but not adenosine triggers preconditioning through PI3-kinase and a tyrosine kinase. American Journal of Physiology. Heart and Circulatory Physiology 284 (2), H727–H734, 2003.

Richard V, Blanc T, Kaeffer N, Tron C, Thuillez C. Myocardial and coronary endothelial protective effects of acetylcholine after myocardial ischaemia and reperfusion in rats: Role of nitric oxide. British Journal of Pharmacology 115 (8), 1532–1538, 1995.

Shimizu S, Akiyama T, Kawada T, Shishido T, Yamazaki T, Kamiya A, Mizuno M, Sano S, Sugimachi M. In vivo direct monitoring of vagal acetylcholine release to the sinoatrial node. Autonomic Neuroscience: Basic and Clinical 148 (1–2), 44–49, 2009.

Snedecor GW, Cochran WG. Statistical Methods. Iowa State, Iowa, pp. 290–291, 1989.

Ståhle L. The use of microdialysis in pharmacokinetics and pharmacodynamics. In: Robinson, TE, JusticeJr. Jr, JB (Eds.), Microdialysis in the Neurosciences, pp. 155–174. Elsevier Science Ltd. New York, 1991.

Thames MD, Klopfenstein HS, Abboud FM, Mark AL, Walker JL. Preferential distribution of inhibitory cardiac receptors with vagal afferents to the inferoposterior wall of the left ventricle activated during coronary occlusion in the dog. Circulation Research 43 (4), 512–519, 1978.

Uemura K, Li M, Tsutsumi T, Yamazaki T, Kawada T, Kamiya A, Inagaki M, Sunagawa K, Sugimachi M. Efferent vagal nerve stimulation induces tissue inhibitor of metalloproteinase-1 in myocardial ischemia–reperfusion injury in rabbit. American Journal of Physiology. Heart and Circulatory Physiology 293 (4), H2254–H2261, 2007.

Vanoli E, de Ferrari GM, Stramba-Badiale M, Hull Jr SS, Foreman RD, Schwartz PJ. Vagal stimulation and prevention of sudden death in conscious dogs with a healed myocardial infarction. Circulation Research 68 (5), 1471–1481, 1991.

Yao Z, Gross GJ. Acetylcholine mimics ischemic preconditioning via a glibenclamide-sensitive mechanism in dogs. American Journal of Physiology 264 (6 Pt 2), H2221–H2225, 1993.